Klimaänderung II
6. Kurzlebige Klimaantriebe

Robert Sausen

Institut für Physik der Atmosphäre
Deutsches Zentrum für Luft- und Raumfahrt
Oberpfaffenhofen

Vorlesung SS 2022

LMU München

Klausur

- **Theresienstr. 39, B 040**
- **20.07.2023, 14:15**
- **Dauer: 2 h**

Technical information

- http://www.pa.op.dlr.de/~RobertSausen/vorlesung/index.html
  - Most recent update on the lecture
  - Slides of the lecture (with some delay)

  - See also LSF https://lsf.verwaltung.uni-muenchen.de/

- Contact: robert.sausen@dlr.de

- Further information:
  - www.ipcc.ch
  - www.de-ipcc.de

Contents of IPCC AR 6 2021
Working Group I: the Physical Science Basis

Chapters

Chapter 1: Framing, context, methods	DOWNLOAD
Chapter 2: Changing state of the climate system	DOWNLOAD
Chapter 3: Human influence on the climate system	DOWNLOAD
Chapter 4: Future global climate: scenario-based projections and near-term information	DOWNLOAD
Chapter 5: Global carbon and other biogeochemical cycles and feedbacks	DOWNLOAD
Chapter 6: Short-lived climate forcers	DOWNLOAD
Chapter 7: The Earth's energy budget, climate feedbacks, and climate sensitivity	DOWNLOAD
Chapter 8: Water cycle changes	DOWNLOAD
Chapter 9: Ocean, cryosphere, and sea level change	DOWNLOAD
Chapter 10: Linking global to regional climate change	DOWNLOAD
Chapter 11: Weather and climate extreme events in a changing climate	DOWNLOAD
Chapter 12: Climate change information for regional impact and for risk assessment	DOWNLOAD
Atlas	DOWNLOAD

Supplementary Material

Annexes

https://www.ipcc.ch/report/ar6/wg1/#FullReport

Chapter 6: Short-lived Climate Forcers

Coordinating Lead Authors:

Sophie Szopa (France), Vaishali Naik (United States of America)

Lead Authors:

Bhupesh Adhikary (Nepal), Paulo Artaxo (Brazil), Terje Berntsen (Norway), William D. Collins (United States of America), Sandro Fuzzi (Italy), Laura Gallardo (Chile), Astrid Kiendler-Scharr (Germany/Austria), Zbigniew Klimont (Austria/Poland), Hong Liao (China), Nadine Unger (United Kingdom/United States of America), Prodromos Zanis (Greece)

Chapter 6: Short-lived Climate Forcers

Contributing Authors:

Wenche Aas (Norway), Dimitris Akritidis (Greece), Robert J. Allen (United States of America), Nicolas Bellouin (United Kingdom/France),Sophie Berger (France/Belgium),Sara M.Blichner (Norway), Josep G. Canadell (Australia), William Collins (United Kingdom), Owen R. Cooper (United States of America), Frank J. Dentener (EU/The Netherlands), Sarah Doherty (United States of America), Jean-Louis Dufresne (France), Sergio Henrique Faria (Spain/Brazil), Piers Forster (United Kingdom), Tzung-May Fu (China), Jan S. Fuglestvedt (Norway), John C. Fyfe (Canada),Aristeidis K. Georgoulias (Greece), Matthew J. Gidden (Austria/United States of America), Nathan P. Gillett (Canada), Paul Ginoux (United States of America), Paul T. Griffiths (United Kingdom), Jian He (United States of America/China), Christopher Jones (United Kingdom), Svitlana Krakovska (Ukraine), Chaincy Kuo (United States of America), David S. Lee (United Kingdom), Maurice Levasseur (Canada), Martine Lizotte (Canada), Thomas K. Maycock (United States of America), Jean-François Müller (Belgium), Helène Muri (Norway), Lee T. Murray (United States of America), Zebedee R. J. Nicholls (Australia), Jurgita Ovadnevaite (Ireland/Lithuania), Prabir K. Patra (Japan/India), Fabien Paulot (United States of America/France, United States of America), Pallav Purohit (Austria/India), Johannes Quaas (Germany), Joeri Rogelj (United Kingdom/Belgium), Bjørn H. Samset (Norway), Chris Smith (United Kingdom), Izuru Takayabu (Japan), Marianne Tronstad Lund (Norway), Alexandra P. Tsimpidi (Germany/Greece), Steven Turnock (United Kingdom), Rita Van Dingenen (Italy/Belgium), Hua Zhang (China), Alcide Zhao (United Kingdom/China)

Chapter 6: Short-lived Climate Forcers

Review Editors:

Yugo Kanaya (Japan), Michael J. Prather (United States of America), Noureddine Yassaa (Algeria)

Chapter Scientist:

Chaincy Kuo (United States of America)

Evaluation and communication of degree of certainty in AR6 findings

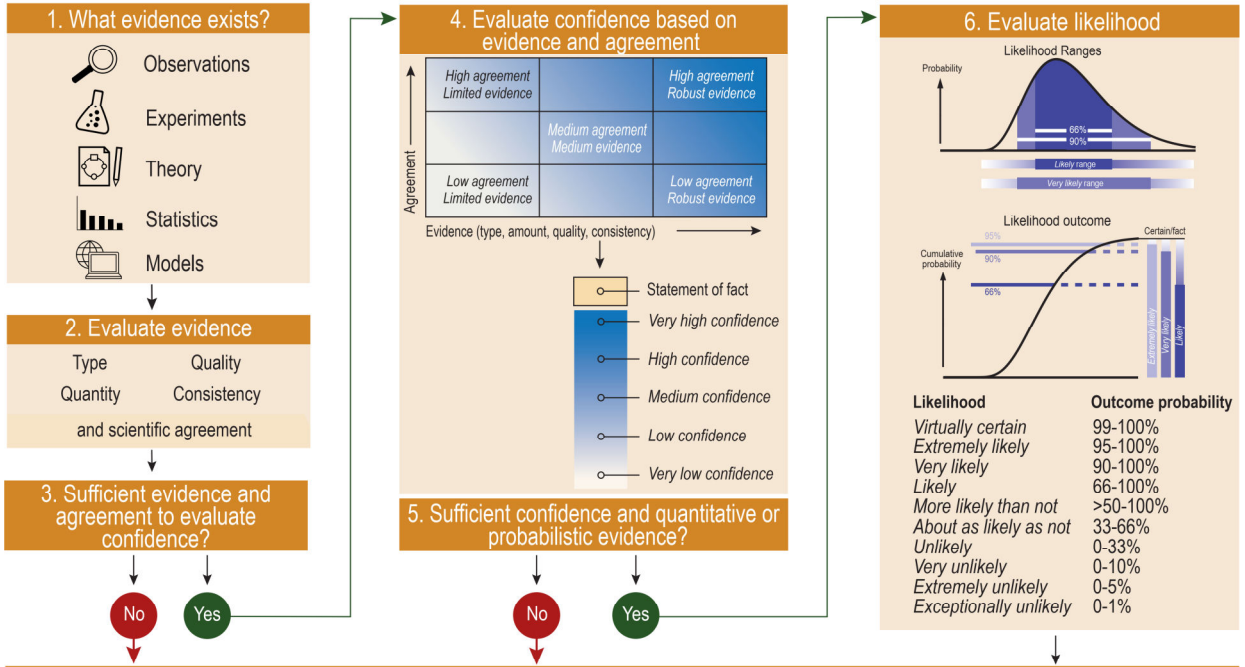

Examples of assessments

Assessed evidence and agreement

Past projections of global temperature and the pattern of warming are broadly consistent with subsequent observations (*limited evidence, high agreement*) {1.3.6}.

Assessed fact

It is unequivocal that human influence has warmed the atmosphere, ocean and land. Widespread and rapid changes in the atmosphere, ocean, cryosphere and biosphere have occurred. {SPM.A.1}

Assessed confidence

The probability of low-likelihood, high impact outcomes increases with higher global warming levels (*high confidence*). {SPM.C.3.2}

The last time global surface temperature was sustained at or above 2.5°C higher than 1850–1900 was over 3 million years ago (*medium confidence*). {SPM.B.1.1}

There is *low confidence* in long-term (multi-decadal to centennial) trends in the frequency of all-category tropical cyclones. {SPM.A.3.4}

Assessed likelihood

It is *virtually certain* that hot extremes (including heatwaves) have become more frequent and more intense across most land regions since the 1950s... {SPM.A.3.1}

Based on multiple lines of evidence, the *very likely* range of equilibrium climate sensitivity is between 2°C (*high confidence*) and 5°C (*medium confidence*). The AR6 assessed best estimate is 3°C with a *likely* range of 2.5°C to 4°C (*high confidence*)... {SPM.A.4.4}

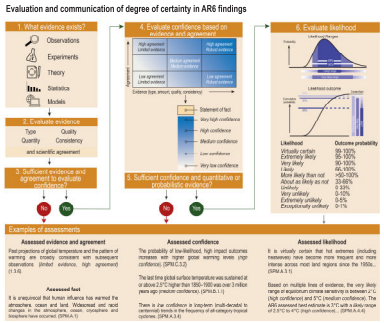

4. Evaluate confidence based on evidence and agreement

Agreement \ Evidence (type, amount, quality, consistency)		
		High agreement Robust evidence
	Medium agreement Medium evidence	
Low agreement Limited evidence		Low agreement Robust evidence

- Statement of fact
- Very high confidence
- High confidence
- Medium confidence
- Low confidence
- Very low confidence

5. Sufficient confidence and quantitative or probabilistic evidence?

- No
- Yes

6. Evaluate likelihood

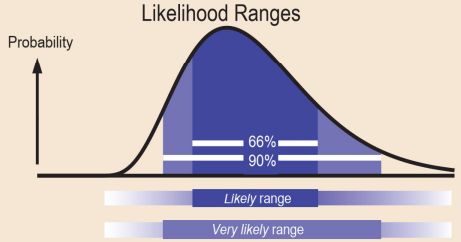

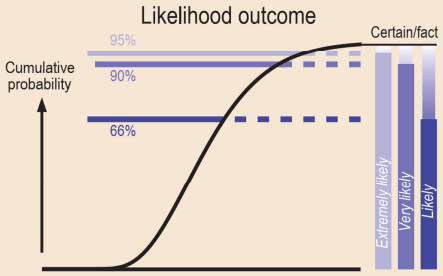

Likelihood	Outcome probability
Virtually certain	99-100%
Extremely likely	95-100%
Very likely	90-100%
Likely	66-100%
More likely than not	>50-100%
About as likely as not	33-66%
Unlikely	0-33%
Very unlikely	0-10%
Extremely unlikely	0-5%
Exceptionally unlikely	0-1%

IPCC 2021, Chap. 1

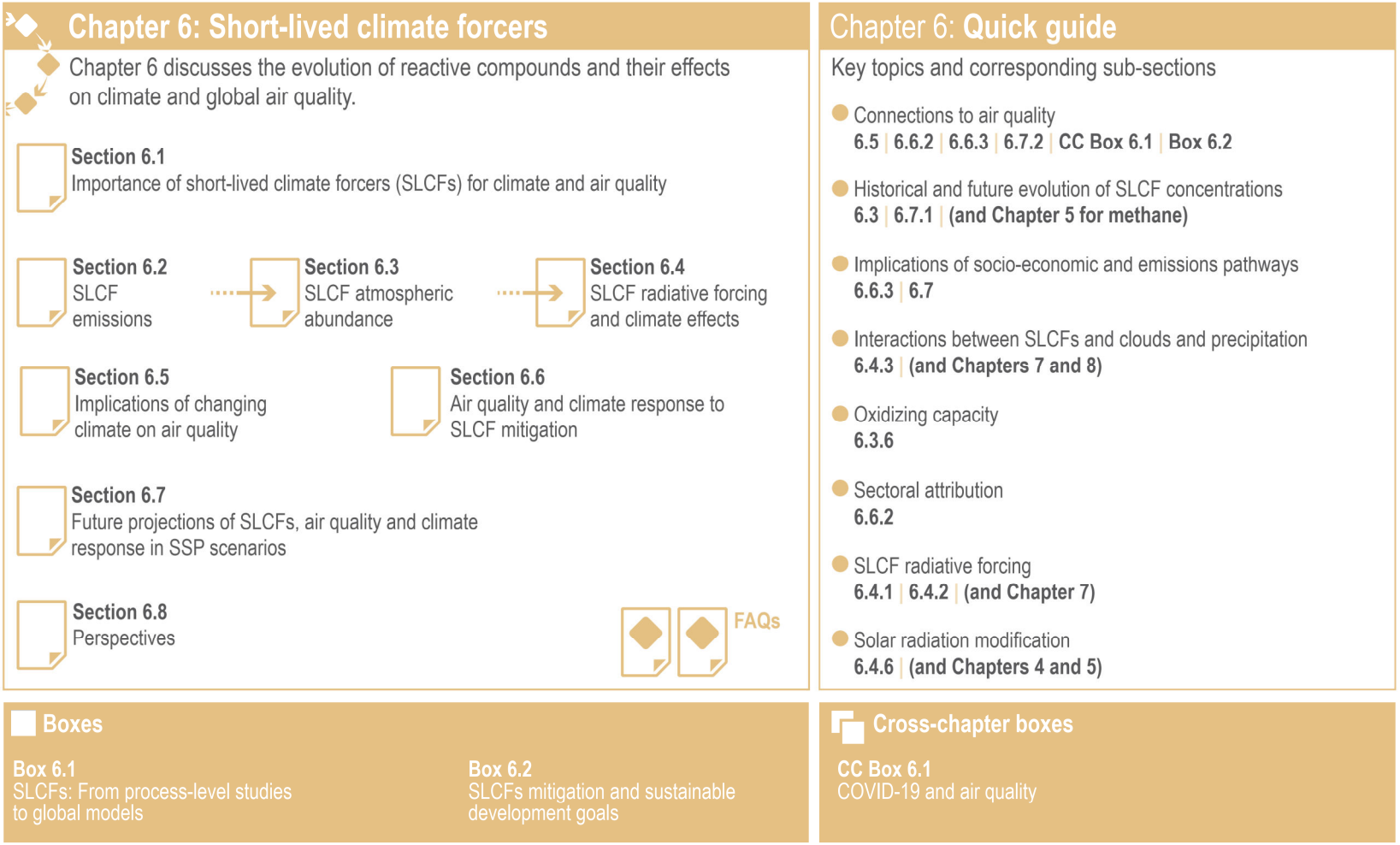

Figure 6.2 | Visual guide to Chapter 6. See Section 6.1.3 for additional description of the chapter.

Statements in the Executive Summary

Short-lived climate forcers (SLCFs) affect climate and are, in most cases, also air pollutants. They include aerosols (sulphate, nitrate, ammonium, carbonaceous aerosols, mineral dust and sea spray), which are also called particulate matter (PM), and chemically reactive gases (methane, ozone, some halogenated compounds, nitrogen oxides, carbon monoxide, non-methane volatile organic compounds, sulphur dioxide and ammonia).

IPCC 2021, Chap. 6

Statements in the Executive Summary

Short-lived climate forcers (SLCFs) affect climate and are, in most cases, also air pollutants. They include aerosols (sulphate, nitrate, ammonium, carbonaceous aerosols, mineral dust and sea spray), which are also called particulate matter (PM), and chemically reactive gases (methane, ozone, some halogenated compounds, nitrogen oxides, carbon monoxide, non-methane volatile organic compounds, sulphur dioxide and ammonia). Except for methane and some halogenated compounds whose lifetimes are about a decade or more, SLCF abundances are spatially highly heterogeneous since they only persist in the atmosphere from a few hours to a couple of months. SLCFs are either radiatively active or influence the abundances of radiatively active compounds through chemistry (chemical adjustments), and their climate effect occurs predominantly in the first two decades after their emission or formation.

IPCC 2021, Chap. 6

Statements in the Executive Summary

Short-lived climate forcers (SLCFs) affect climate and are, in most cases, also air pollutants. They include aerosols (sulphate, nitrate, ammonium, carbonaceous aerosols, mineral dust and sea spray), which are also called particulate matter (PM), and chemically reactive gases (methane, ozone, some halogenated compounds, nitrogen oxides, carbon monoxide, non-methane volatile organic compounds, sulphur dioxide and ammonia). Except for methane and some halogenated compounds whose lifetimes are about a decade or more, SLCF abundances are spatially highly heterogeneous since they only persist in the atmosphere from a few hours to a couple of months. SLCFs are either radiatively active or influence the abundances of radiatively active compounds through chemistry (chemical adjustments), and their climate effect occurs predominantly in the first two decades after their emission or formation. They can have either a cooling or warming effect on climate, and they also affect precipitation and other climate variables. Methane and some halogenated compounds are included in climate treaties, unlike the other SLCFs that are nevertheless indirectly affected by climate change mitigation since many of them are often co-emitted with CO_2 in combustion processes.

IPCC 2021, Chap. 6

Statements in the Executive Summary

Short-lived climate forcers (SLCFs) affect climate and are, in most cases, also air pollutants. They include aerosols (sulphate, nitrate, ammonium, carbonaceous aerosols, mineral dust and sea spray), which are also called particulate matter (PM), and chemically reactive gases (methane, ozone, some halogenated compounds, nitrogen oxides, carbon monoxide, non-methane volatile organic compounds, sulphur dioxide and ammonia). Except for methane and some halogenated compounds whose lifetimes are about a decade or more, SLCF abundances are spatially highly heterogeneous since they only persist in the atmosphere from a few hours to a couple of months. SLCFs are either radiatively active or influence the abundances of radiatively active compounds through chemistry (chemical adjustments), and their climate effect occurs predominantly in the first two decades after their emission or formation. They can have either a cooling or warming effect on climate, and they also affect precipitation and other climate variables. Methane and some halogenated compounds are included in climate treaties, unlike the other SLCFs that are nevertheless indirectly affected by climate change mitigation since many of them are often co-emitted with CO_2 in combustion processes. This chapter assesses the changes, in the past and in a selection of possible futures, of the emissions and abundances of individual SLCFs primarily on global to continental scales, and how these changes affect the Earth's energy balance through radiative forcing and feedback in the climate system. The attribution of climate and air-quality changes to emissions sectors and regions, and the effects of SLCF mitigations defined for various environmental purposes, are also assessed.

IPCC 2021, Chap. 6

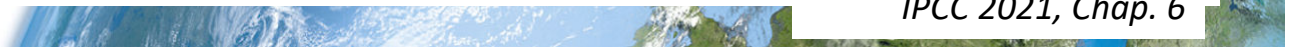

Statements in the Executive Summary

Short-lived climate forcers (SLCFs) affect climate and are, in most cases, also air pollutants. They include aerosols (sulphate, nitrate, ammonium, carbonaceous aerosols, mineral dust and sea spray), which are also called particulate matter (PM), and chemically reactive gases (methane, ozone, some halogenated compounds, nitrogen oxides, carbon monoxide, non-methane volatile organic compounds, sulphur dioxide and ammonia). Except for methane and some halogenated compounds whose lifetimes are about a decade or more, SLCF abundances are spatially highly heterogeneous since they only persist in the atmosphere from a few hours to a couple of months. SLCFs are either radiatively active or influence the abundances of radiatively active compounds through chemistry (chemical adjustments), and their climate effect occurs predominantly in the first two decades after their emission or formation. They can have either a cooling or warming effect on climate, and they also affect precipitation and other climate variables. Methane and some halogenated compounds are included in climate treaties, unlike the other SLCFs that are nevertheless indirectly affected by climate change mitigation since many of them are often co-emitted with CO_2 in combustion processes. This chapter assesses the changes, in the past and in a selection of possible futures, of the emissions and abundances of individual SLCFs primarily on global to continental scales, and how these changes affect the Earth's energy balance through radiative forcing and feedback in the climate system. The attribution of climate and air-quality changes to emissions sectors and regions, and the effects of SLCF mitigations defined for various environmental purposes, are also assessed.

IPCC 2021, Chap. 6

Sources and processes leading to atmospheric short-lived climate forcer (SLCF) burden and their interactions with the climate system

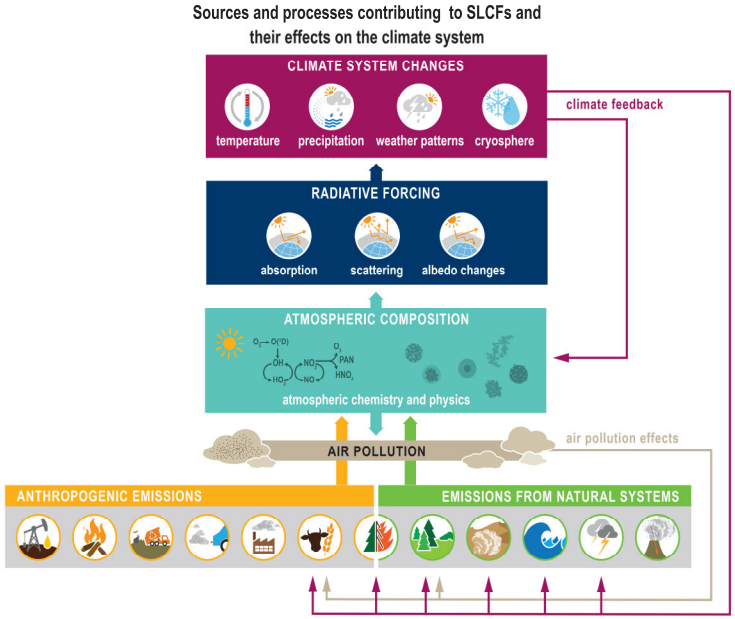

Figure 6.1 | Sources and processes leading to atmospheric short-lived climate forcer (SLCF) burden and their interactions with the climate system. Both direct and indirect SLCFs and the role of atmospheric processes for the lifetime of SLCFs are depicted. Anthropogenic emissions sectors illustrated are: fossil fuel exploration, distribution and use; biofuel production and use; waste; transport; industry; agricultural sources; and open biomass burning. Emissions from natural systems include those from open biomass burning, vegetation, soil, ocean, lightning and volcanoes. SLCFs interact with solar or terrestrial radiation, surface albedo, and cloud or precipitation systems. The radiative forcing due to individual SLCFs can be either positive or negative. Climate change induces changes in emissions from most natural systems as well as from some anthropogenic emissions sectors (e.g., agriculture) leading to a climate feedback (purple arrows). Climate change also influences atmospheric chemistry processes, such as chemical reaction rates or via circulation changes, thus affecting atmospheric composition leading to a climate feedback. Air pollutants influence emissions from terrestrial vegetation, including agriculture (grey arrow).

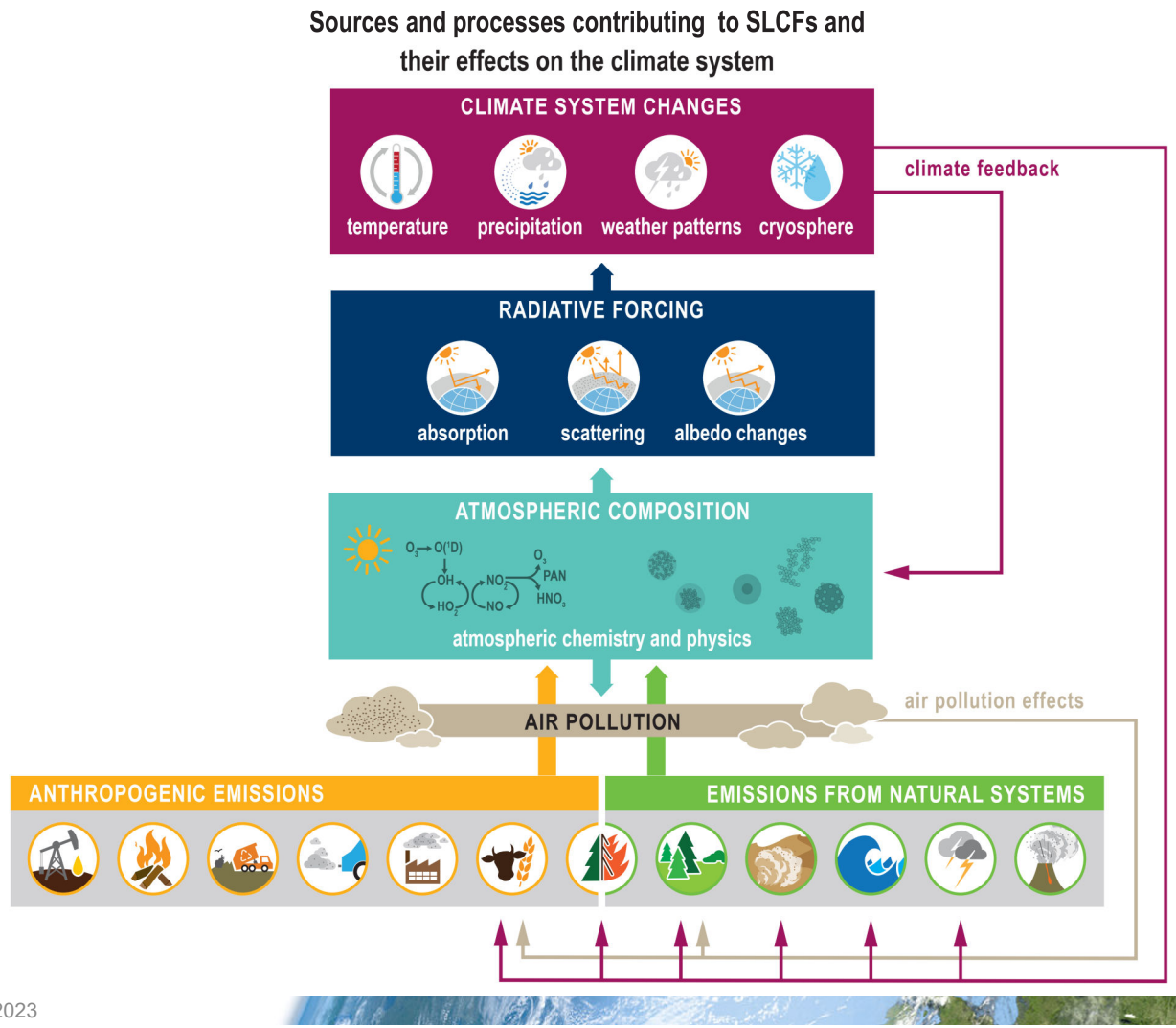
Sources and processes contributing to SLCFs and their effects on the climate system
CLIMATE SYSTEM CHANGES
temperature
precipitation
weather patterns
cryosphere
climate feedback
RADIATIVE FORCING
absorption
scattering
albedo changes
ATMOSPHERIC COMPOSITION
atmospheric chemistry and physics
AIR POLLUTION
air pollution effects
ANTHROPOGENIC EMISSIONS
EMISSIONS FROM NATURAL SYSTEMS

Was ist der "Strahlungsantrieb"? (vereinfacht)
What is "radiative forcing"? (simplified)

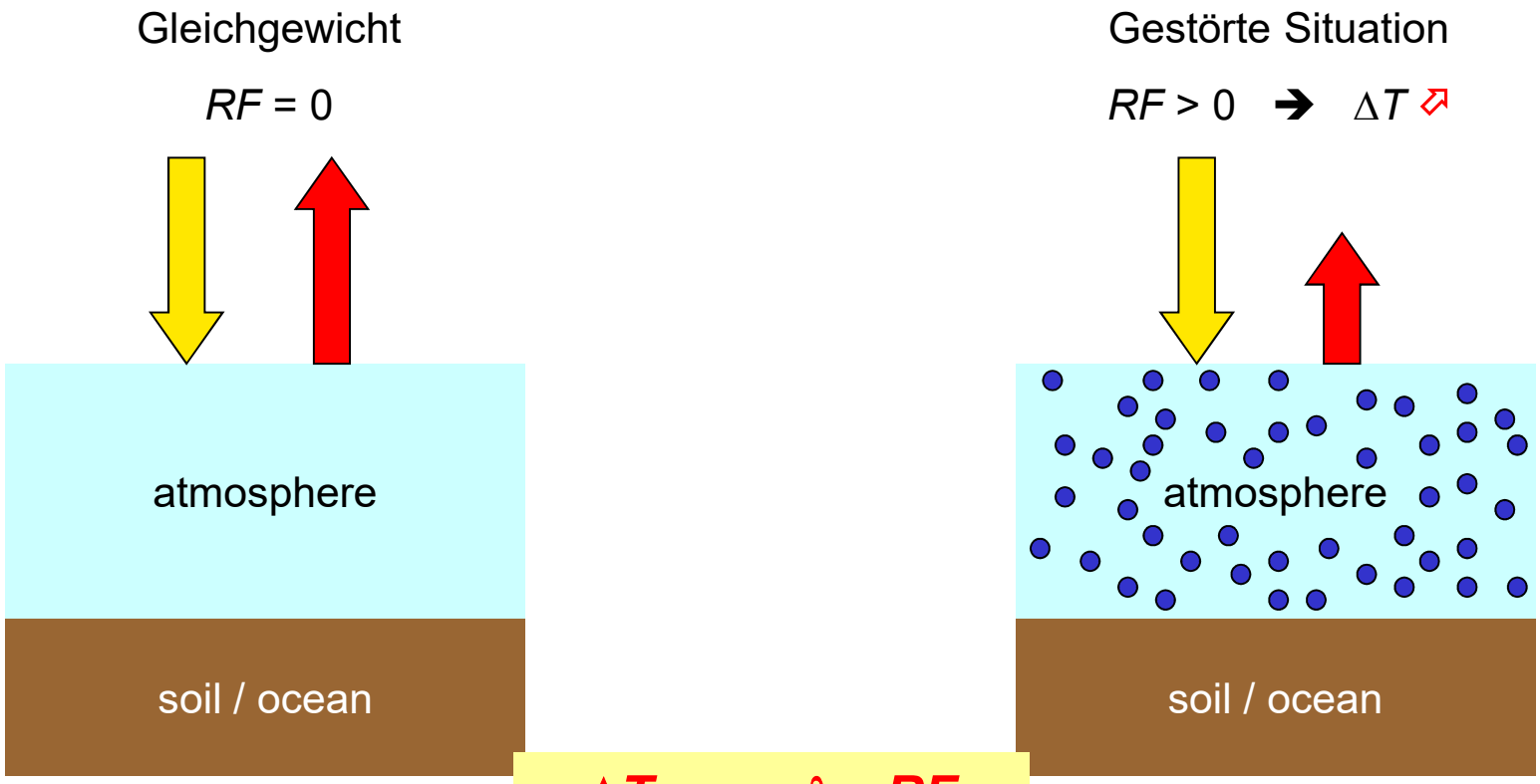

Forcing, Response and Feedback

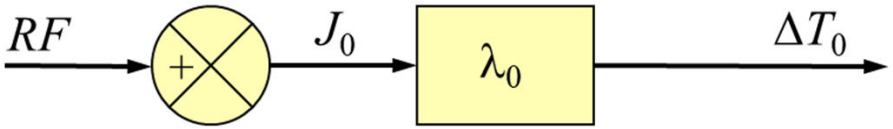

$$\Delta T_0 = \lambda_0 \cdot J_0 = \lambda_0 \cdot RF$$

Example: Albedo feedback

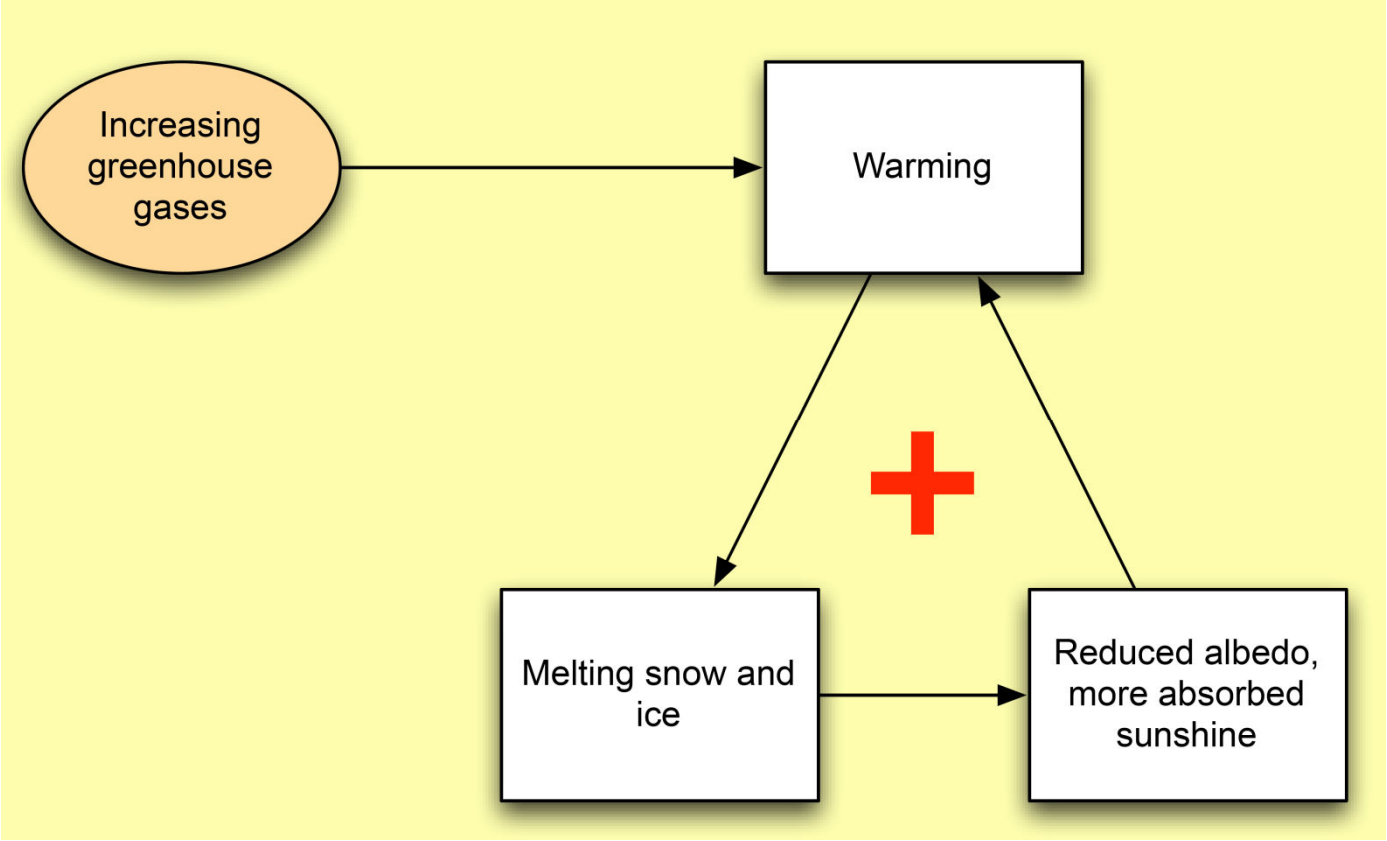

Randel, CSU, 2007

Forcing, Response and Feedback

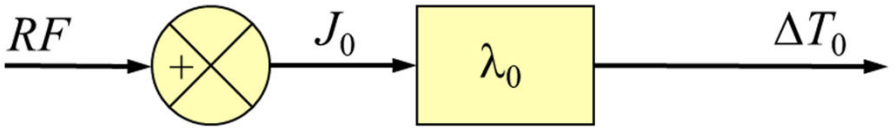

$$\Delta T_0 = \lambda_0 \cdot J_0 = \lambda_0 \cdot RF$$

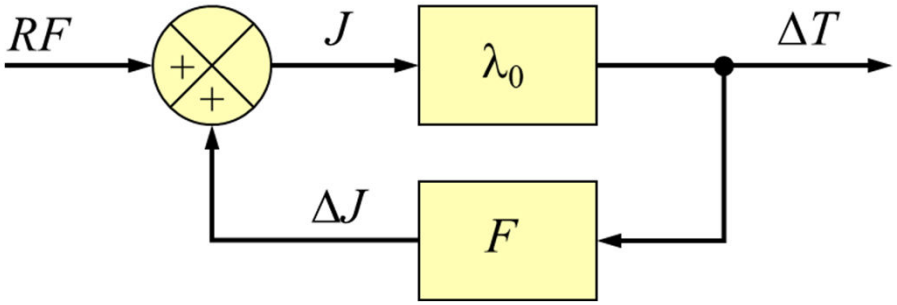

$$J = RF + \Delta J = RF + F \cdot \Delta T$$

$$\Delta T = \lambda_0 \cdot J = \lambda_0 \cdot (RF + F \cdot \Delta T) = \lambda \cdot RF$$

climate sensitivity parameter: λ

ratio of responses: $r = \Delta T / \Delta T_0 = \lambda_0 / \lambda = 1 / (1 - f)$

feedback factor: $f = F \cdot \lambda_0$

feedback: F

Schematic comparing RF calculation methodologies

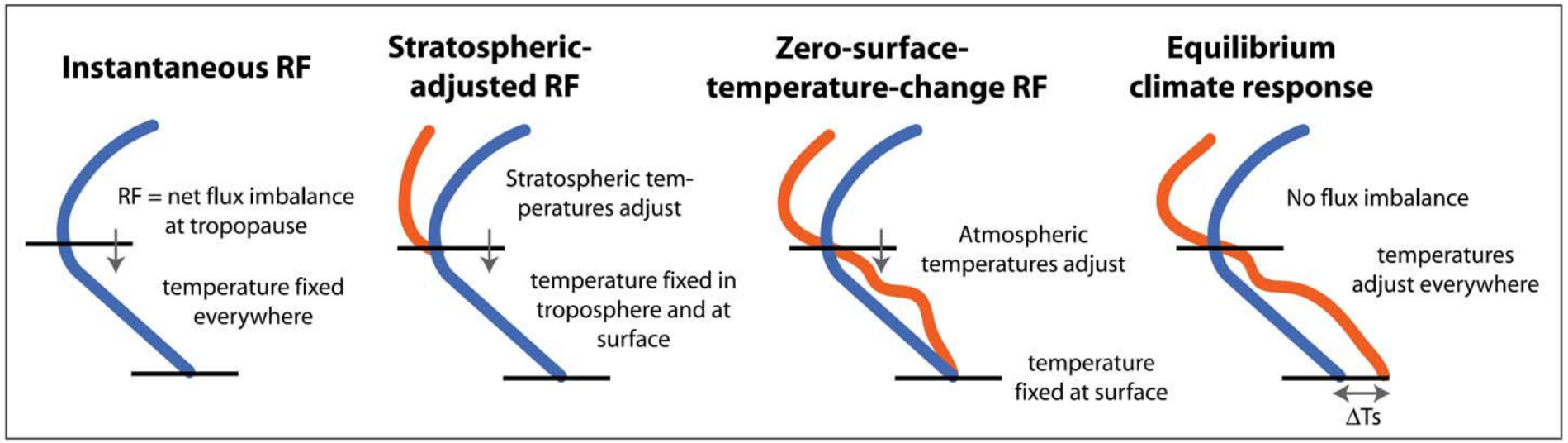

Figure 2.2. *Schematic comparing RF calculation methodologies. Radiative forcing, defined as the net flux imbalance at the tropopause, is shown by an arrow. The horizontal lines represent the surface (lower line) and tropopause (upper line). The unperturbed temperature profile is shown as the blue line and the perturbed temperature profile as the red line. From left to right: Instantaneous RF: atmospheric temperatures are fixed everywhere; stratospheric-adjusted RF: allows stratospheric temperatures to adjust; zero-surface-temperature-change RF: allows atmospheric temperatures to adjust everywhere with surface temperatures fixed; and equilibrium climate response: allows the atmospheric and surface temperatures to adjust to reach equilibrium (no tropopause flux imbalance), giving a surface temperature change (ΔT_s).*

Figure 2.2. *Schematic comparing RF calculation methodologies. Radiative forcing, defined as the net flux imbalance at the tropopause, is shown by an arrow. The horizontal lines represent the surface (lower line) and tropopause (upper line). The unperturbed temperature profile is shown as the blue line and the perturbed temperature profile as the red line. From left to right: Instantaneous RF: atmospheric temperatures are fixed everywhere; stratospheric-adjusted RF: allows stratospheric temperatures to adjust; zero-surface-temperature-change RF: allows atmospheric temperatures to adjust everywhere with surface temperatures fixed; and equilibrium climate response: allows the atmospheric and surface temperatures to adjust to reach equilibrium (no tropopause flux imbalance), giving a surface temperature change (ΔT_s).*

Radiative forcing (RF) and effective radiative forcing (ERF) estimates

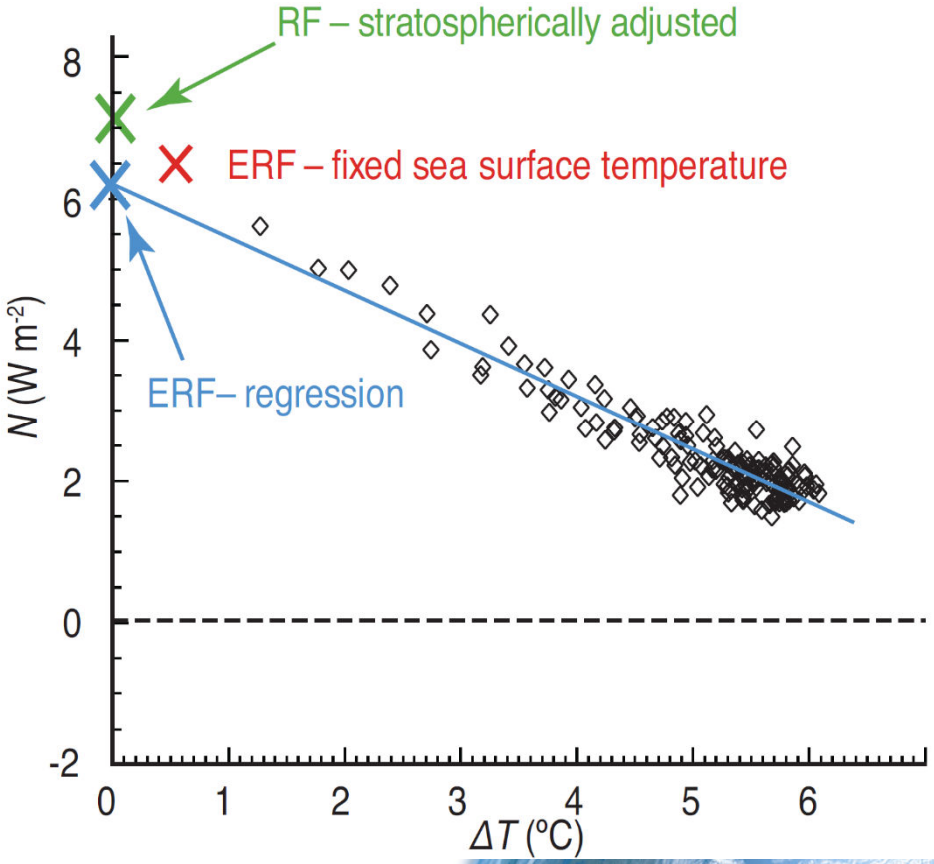

Figure 7.2 | Radiative forcing (RF) and effective radiative forcing (ERF) estimates derived by two methods, for the example of 4 × CO_2 experiments in one climate model. *N* is the net energy imbalance at the top of the atmosphere and ΔT the global mean surface temperature change. The fixed sea surface temperature ERF estimate is from an atmosphere–land model averaged over 30 years. The regression estimate is from 150 years of a coupled model simulation after an instantaneous quadrupling of CO_2, with the *N* from individual years in this regression shown as black diamonds. The stratospherically adjusted RF is the tropopause energy imbalance from otherwise identical radiation calculations at 1 × and 4 × CO_2 concentrations. (Figure follows Andrews et al., 2012.) See also Figure 8.1.

IPCC 2013, Chap. 7

Statements in the Executive Summary

Recent Evolution in Short-lived Climate Forcer (SLCF) (1)

Over the last decade (2010–2019), strong shifts in the geographical distribution of emissions have led to changes in atmospheric abundances of highly variable SLCFs (high confidence). Evidence from satellite and surface observations shows strong regional variations in trends of ozone (O_3), aerosols and their precursors (*high confidence*).

IPCC 2021, Chap. 6

Statements in the Executive Summary

Recent Evolution in Short-lived Climate Forcer (SLCF) (1)

Over the last decade (2010–2019), strong shifts in the geographical distribution of emissions have led to changes in atmospheric abundances of highly variable SLCFs (high confidence). Evidence from satellite and surface observations shows strong regional variations in trends of ozone (O_3), aerosols and their precursors (*high confidence*). In particular, tropospheric columns of nitrogen dioxide (NO_2) and sulphur dioxide (SO_2) continued to decline over North America and Europe (*high confidence*), and to increase over Southern Asia (*medium confidence*), but have declined over Eastern Asia (*high confidence*). Global carbon monoxide (CO) abundance has continued to decline (*high confidence*). The concentrations of hydrofluorocarbons (HFCs) are increasing (*high confidence*). Global carbonaceous aerosol budgets and trends remain poorly characterized due to limited observations, but sites representative of background conditions have reported multi-year declines in black carbon (BC) over several regions of the Northern Hemisphere. {6.2, 6.3, 2.2.4, 2.2.5, 2.2.6}

IPCC 2021, Chap. 6

Relative regional and sectoral contributions to the present day (year 2014) anthropogenic emissions of short-lived climate forcers (SLCFs)

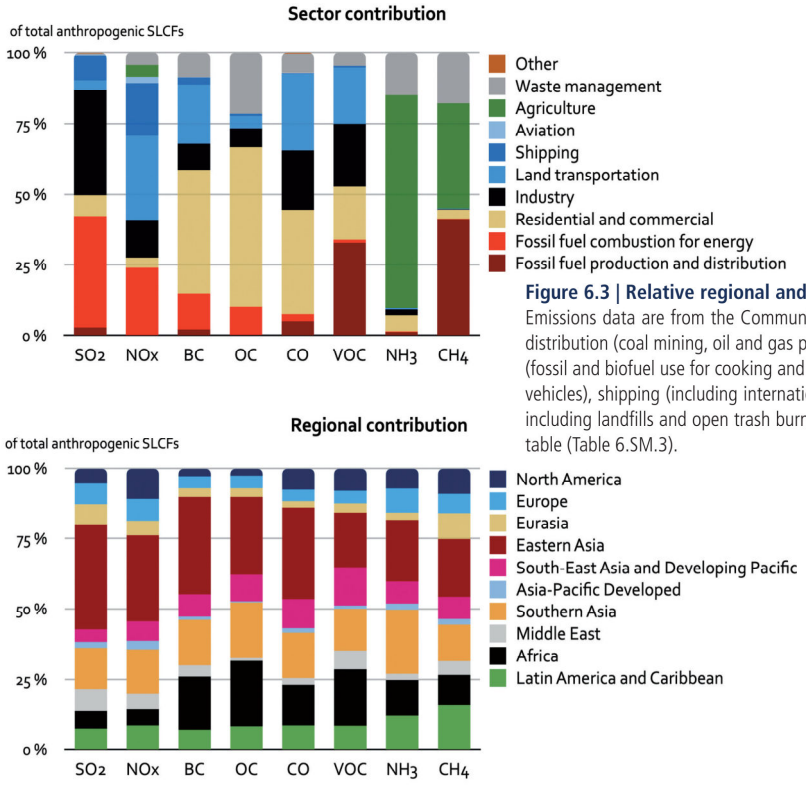

Figure 6.3 | Relative regional and sectoral contributions to the present day (year 2014) anthropogenic emissions of short-lived climate forcers (SLCFs). Emissions data are from the Community Emissions Data System (CEDS; Hoesly et al., 2018). Emissions are aggregated into the following sectors: fossil fuel production and distribution (coal mining, oil and gas production, upstream gas flaring, gas distribution networks), fossil fuel combustion for energy (power plants), residential and commercial (fossil and biofuel use for cooking and heating), industry (combustion and production processes, solvent-use losses from production and end use), transport (road and off-road vehicles), shipping (including international shipping), aviation (including international aviation), agriculture (livestock and crop production), waste management (solid waste, including landfills and open trash burning, residential and industrial waste water), and other. Further details on data sources and processing are available in the chapter data table (Table 6.SM.3).

IPCC 2021, Chap. 6

Relative regional and sectoral contributions to the present day (year 2014) anthropogenic emissions of short-lived climate forcers (SLCFs)

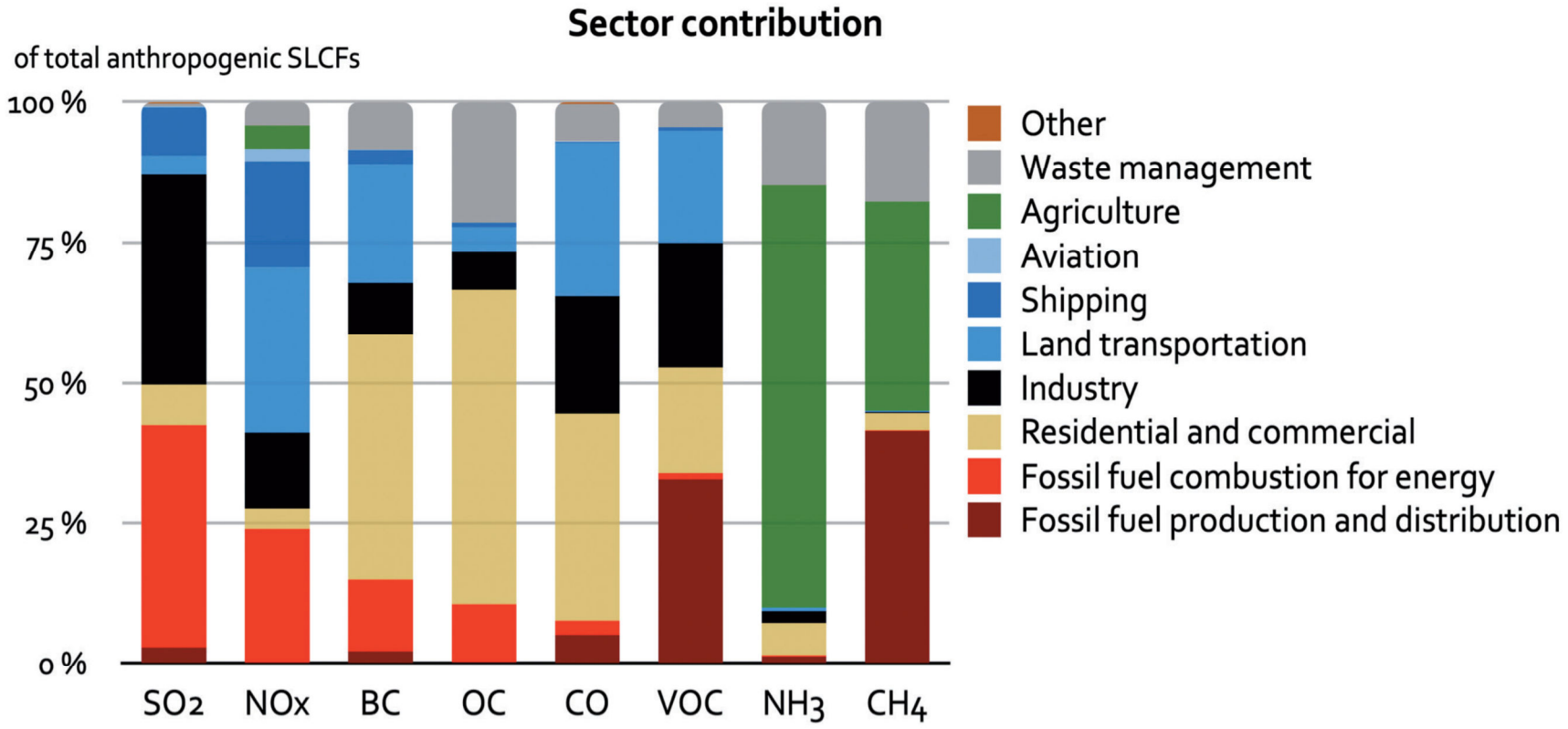

IPCC 2021, Chap. 6

Relative regional and sectoral contributions to the present day (year 2014) anthropogenic emissions of short-lived climate forcers (SLCFs)

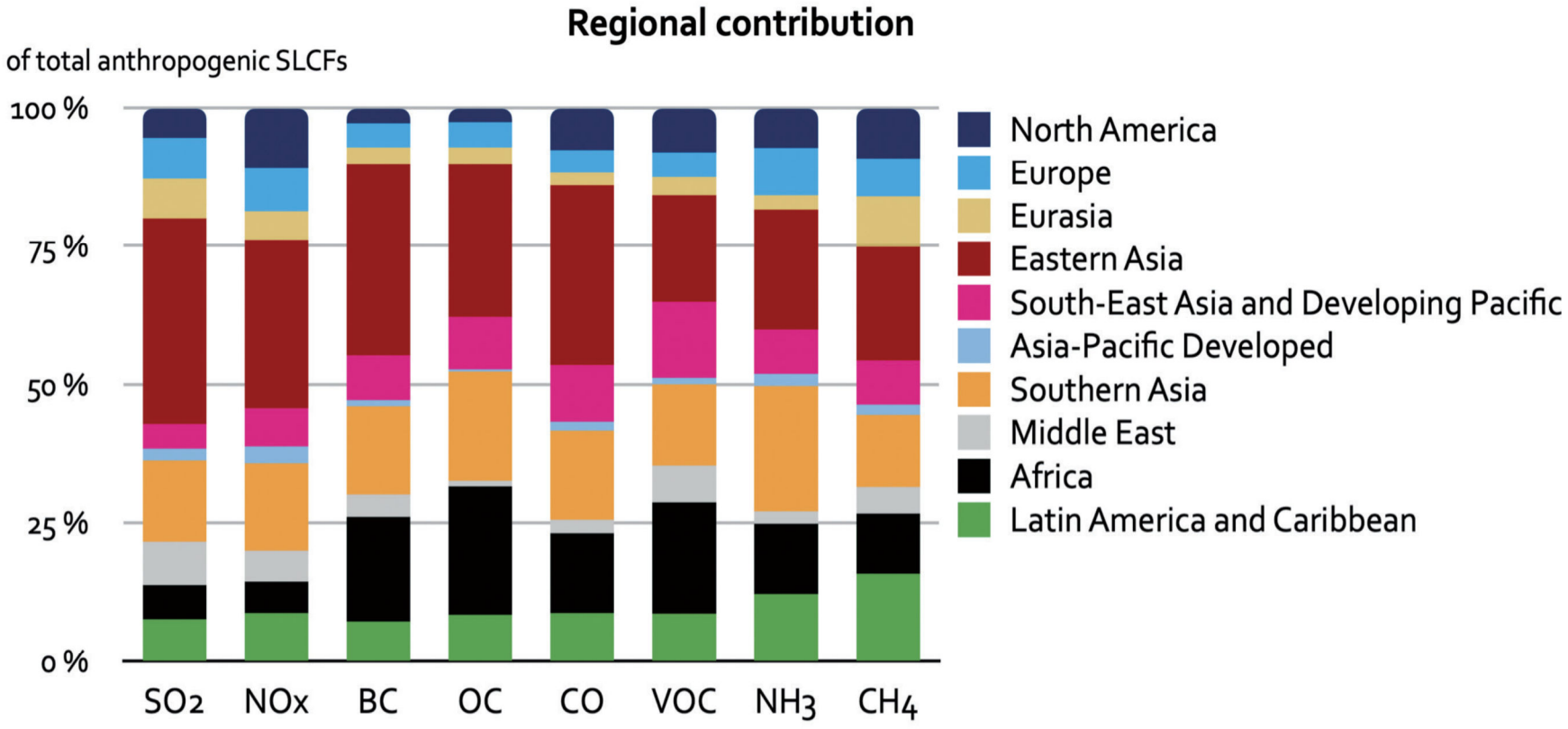

IPCC 2021, Chap. 6

Time evolution of global annual mean tropospheric ozone burden (in Tg) from 1850 to 2100

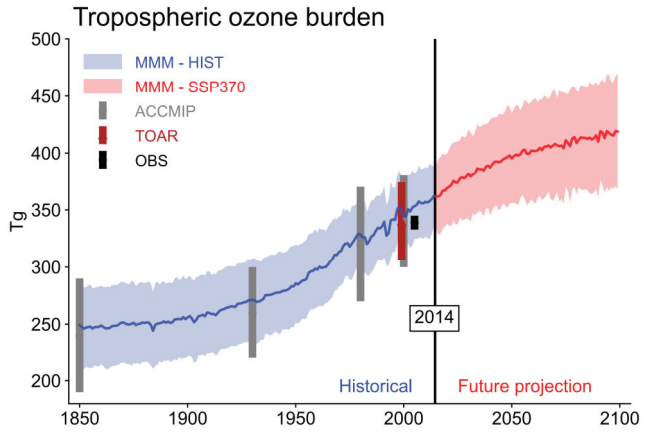

Figure 6.4 | Time evolution of global annual mean tropospheric ozone burden (in Tg) from 1850 to 2100. Multi-model means for CMIP6 historical experiment (1850–2014) from UKESM1-LL-0, CESM2-WACCM, MRI-ESM2-0, GISS-E2.1-G and GFDL-ESM4 and for ScenarioMIP SSP3-7.0 experiment (2015–2100) are represented with their inter-model standard deviation (±1 standard deviation, shaded areas). Observation-based global tropospheric ozone burden estimate (from Table 6.3) is for 2010–2014. Tropospheric Ozone Assessment Report (TOAR) multi-model mean value (from Table 6.3) is for 2000 with a ±1 standard deviation error-bar. Atmospheric Chemistry and Climate Model Intercomparison Project (ACCMIP) multi-model means are for 1850, 1930, 1980 and 2000 time slices with ±1 standard deviation error-bars. The troposphere is masked by the tropopause pressure calculated in each model using the WMO thermal tropopause definition. Further details on data sources and processing are available in the chapter data table (Table 6.SM.3).

IPCC 2021, Chap. 6

Time evolution of global annual mean tropospheric ozone burden (in Tg) from 1850 to 2100

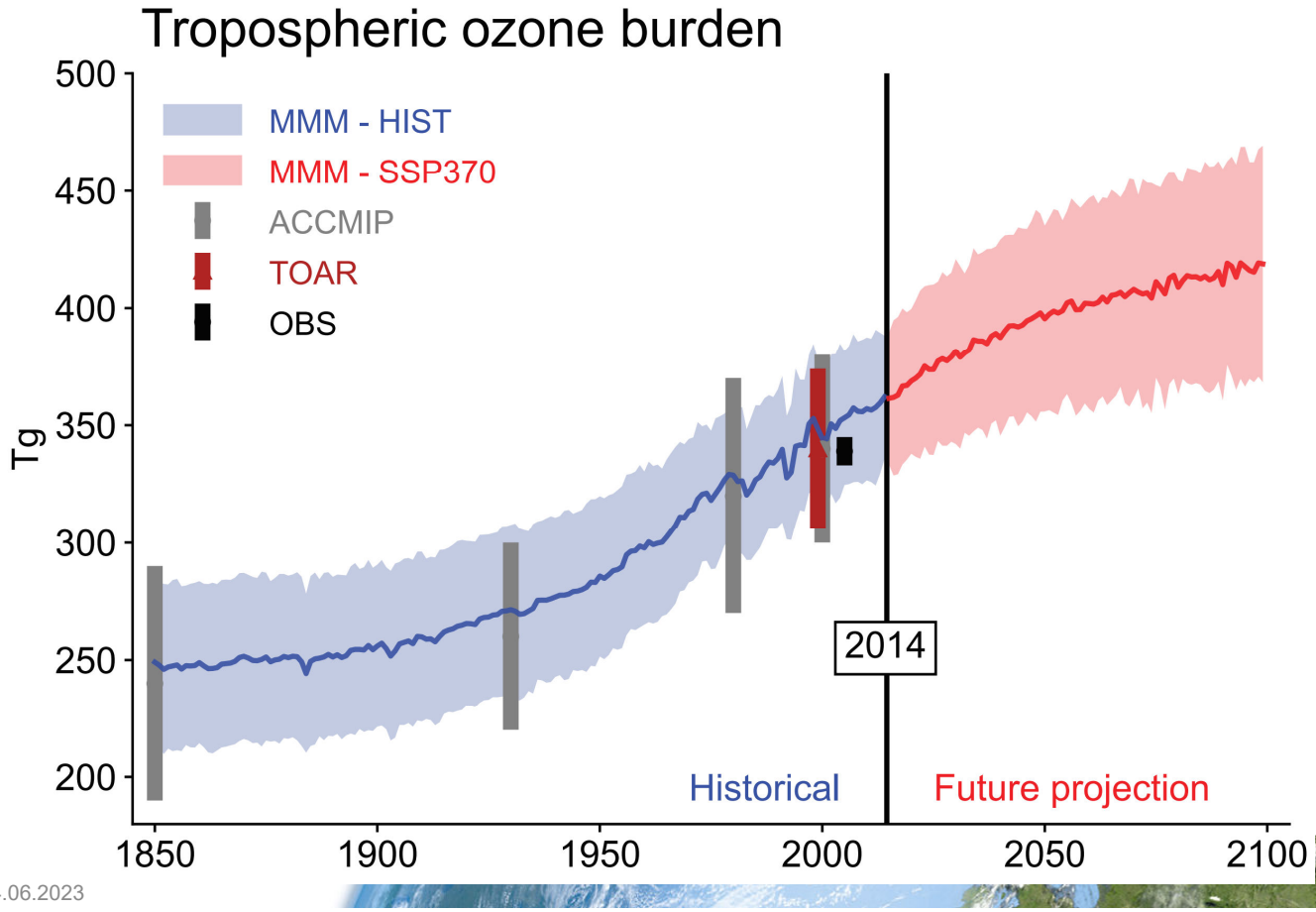

IPCC 2021, Chap. 6

Decadal tropospheric ozone trends since 1994

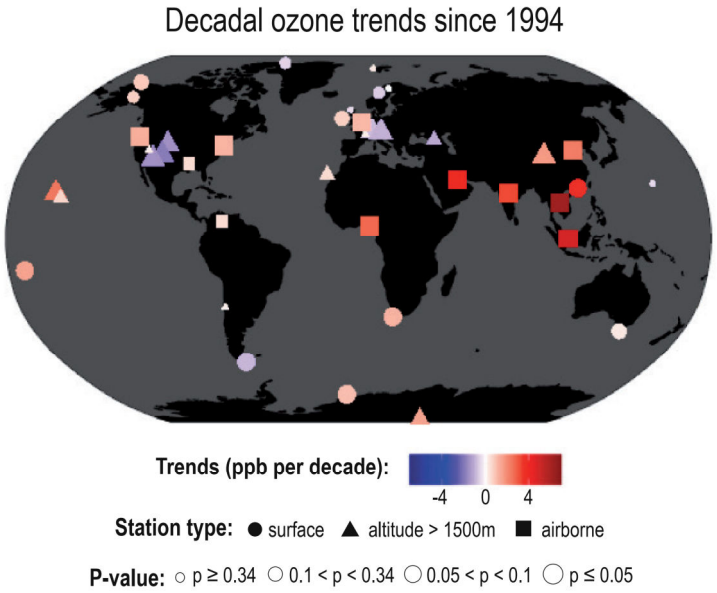

Figure 6.5 | Decadal tropospheric ozone trends since 1994. Trends are shown at 28 remote and regionally representative surface sites (Cooper et al., 2020) and in 11 regions of the lower free troposphere (650 hPa, about 3.5 km) as measured by In-Service Aircraft for a Global Observing System (IAGOS) above Europe, north-eastern USA, south-eastern USA, western North America, north-east China, South East Asia, southern India, the Persian Gulf, Malaysia/Indonesia, the Gulf of Guinea and northern South America (Gaudel et al., 2020). High-elevation surface sites are >1500 m above sea level. All trends end with the most recently available year but begin in 1995 or 1994. The sites and datasets are the same as those used in Figure 2.8, further details on data sources and processing are available in the Chapter 2 data table (Table 2.SM.1).

IPCC 2021, Chap. 6

Decadal tropospheric ozone trends since 1994

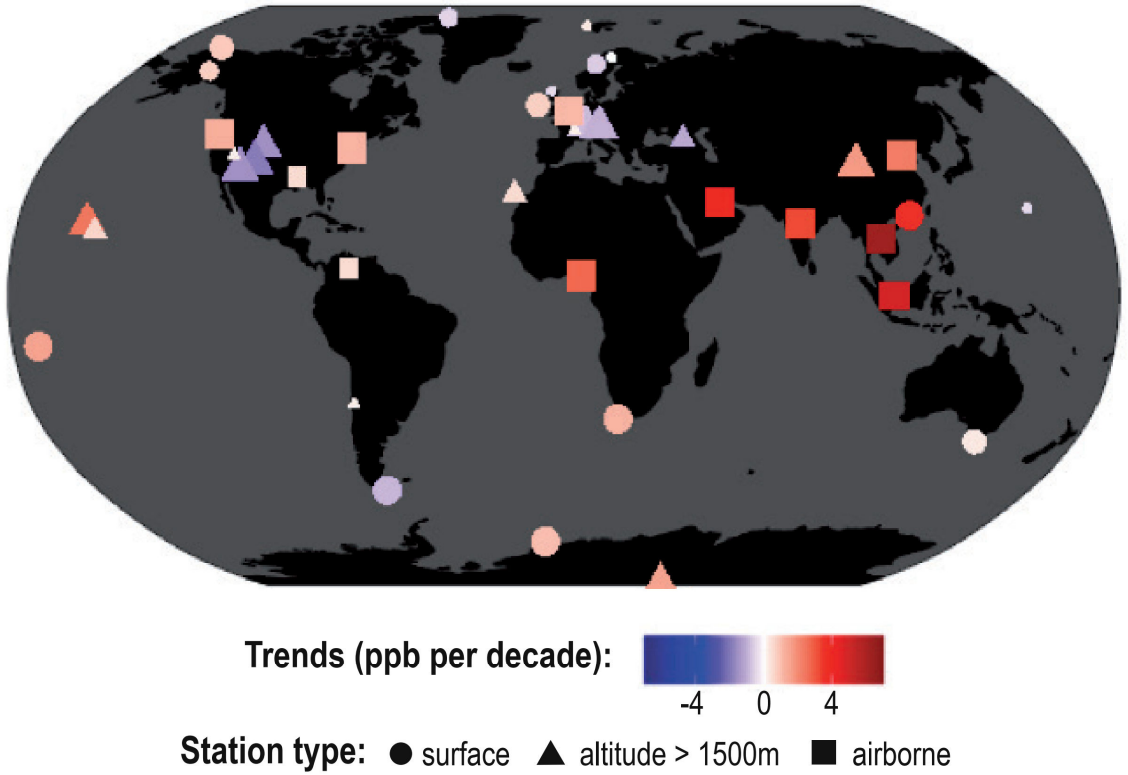

IPCC 2021, Chap. 6

Long-term climatological mean (a) and time evolution (b) of tropospheric nitrogen dioxide (NO_2) vertical column density

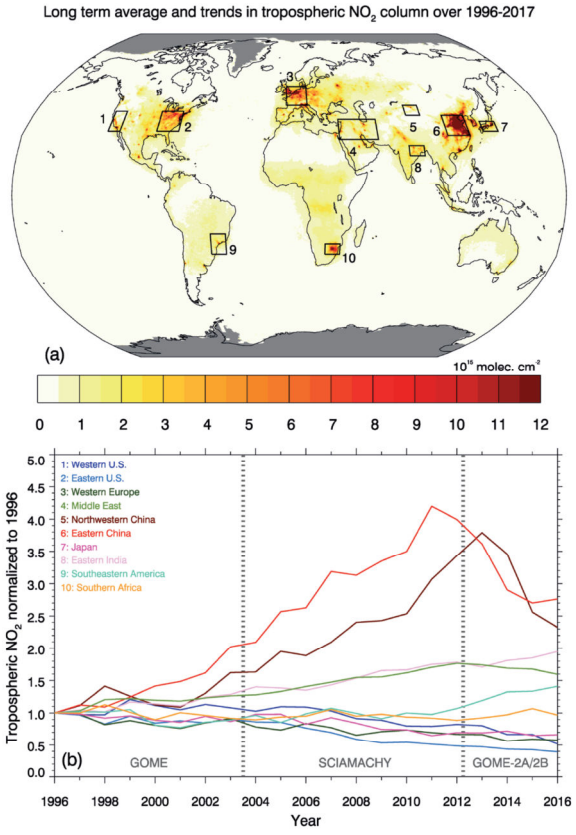

Figure 6.6 | Long-term climatological mean (a) and time evolution (b) of tropospheric nitrogen dioxide (NO_2) vertical column density. Data are from the merged GOME/SCIAMACHY/GOME-2 (TM4NO2A version 2.3) dataset for the period 1996–2016 (Georgoulias et al., 2019). Time evolution of NO_2 column shown in panel (b) is normalized to the fitted 1996 levels for the 10 regions shown as boxes in panel (a). Further details on data sources and processing are available in the chapter data table (Table 6.SM.3).

IPCC 2021, Chap. 6

Long-term climatological mean (a) and time evolution (b) of tropospheric nitrogen dioxide (NO_2) vertical column density

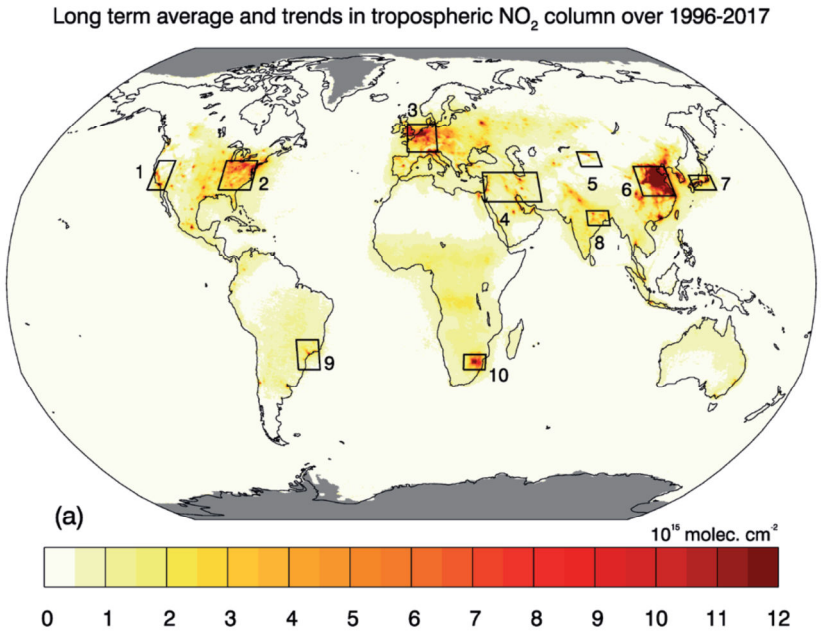

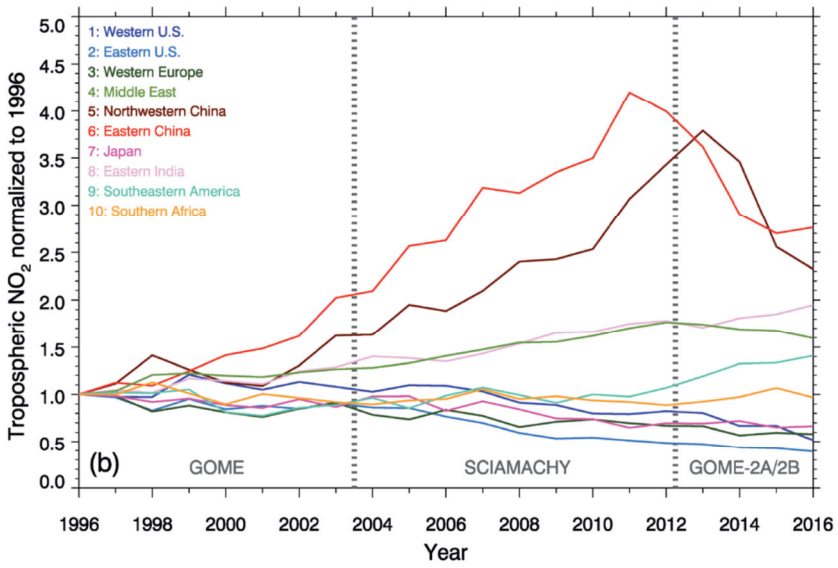

IPCC 2021, Chap. 6

Distribution of PM2.5 composition mass concentration (in µg m^{-3}) for the major PM2.5 aerosol components

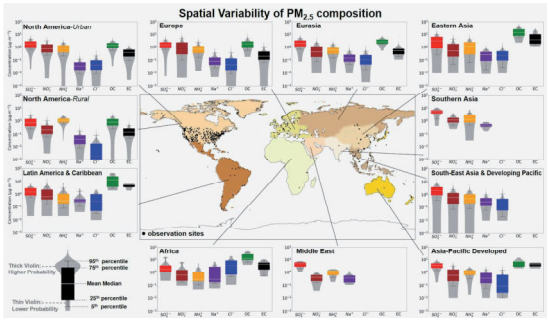

Figure 6.7 | Distribution of $PM_{2.5}$ composition mass concentration (in µg m^{-3}) for the major $PM_{2.5}$ aerosol components. Those aerosol components are sulphate, nitrate, ammonium, sodium, chloride, organic carbon and elemental carbon. The central world map depicts the intermediate-level regional breakdown of observations (10 regions) following the IPCC Sixth Assessment Report Working Group III (AR6 WGIII). Monthly averaged $PM_{2.5}$ aerosol component measurements are from: **(i)** the Environmental Protection Agency (EPA) network which include 211 monitor sites primarily in urban areas of North America during 2000–2018 (Solomon et al., 2014), **(ii)** the Interagency Monitoring of Protected Visual Environments (IMPROVE) network during 2000–2018 over 198 monitoring sites representative of the regional haze conditions over North America, **(iii)** the European Monitoring and Evaluation Programme (EMEP) network over 70 monitoring in Europe and (eastern) Eurasia during 2000–2018, **(iv)** the Acid Deposition Monitoring Network in Eastern Asia (EANET) network with 39 (18 remote, 10 rural, 11 urban) sites in Eurasia, Eastern Asia, South East Asia and Developing Pacific, and Asia-Pacific Developed during 2001–2017, **(v)** the global Surface Particulate Matter Network (SPARTAN) during 2013–2019 with sites primarily in highly populated regions around the world (i.e., North America, Latin America and Caribbean, Africa, Middle East, Southern Asia, Eastern Asia, South East Asia and Developing Pacific; Snider et al., 2015, 2016), and **(vii)** individual observational field campaign averages over Latin America and Caribbean, Africa, Europe, Eastern Asia, and Asia-Pacific Developed (Celis et al., 2004; Feng et al., 2006; Bourotte et al., 2007; Fuzzi et al., 2007; Mariani and de Mello, 2007; Molina et al., 2007, 2010; Favez et al., 2008; Mkoma, 2008; Aggarwal and Kawamura, 2009; Mkoma et al., 2009; de Souza et al., 2010; Li et al., 2010; Martin et al., 2010; Radhi et al., 2010; Weinstein et al., 2010; Batmunkh et al., 2011; Gioda et al., 2011; Pathak et al., 2011; F. Zhang et al., 2012; Cho and Park, 2013; Zhao et al., 2013; Wang et al., 2019; Kuzu et al., 2020). Further details on data sources and processing are available in the chapter data table (Table 6.SM.3).

IPCC 2021, Chap. 6

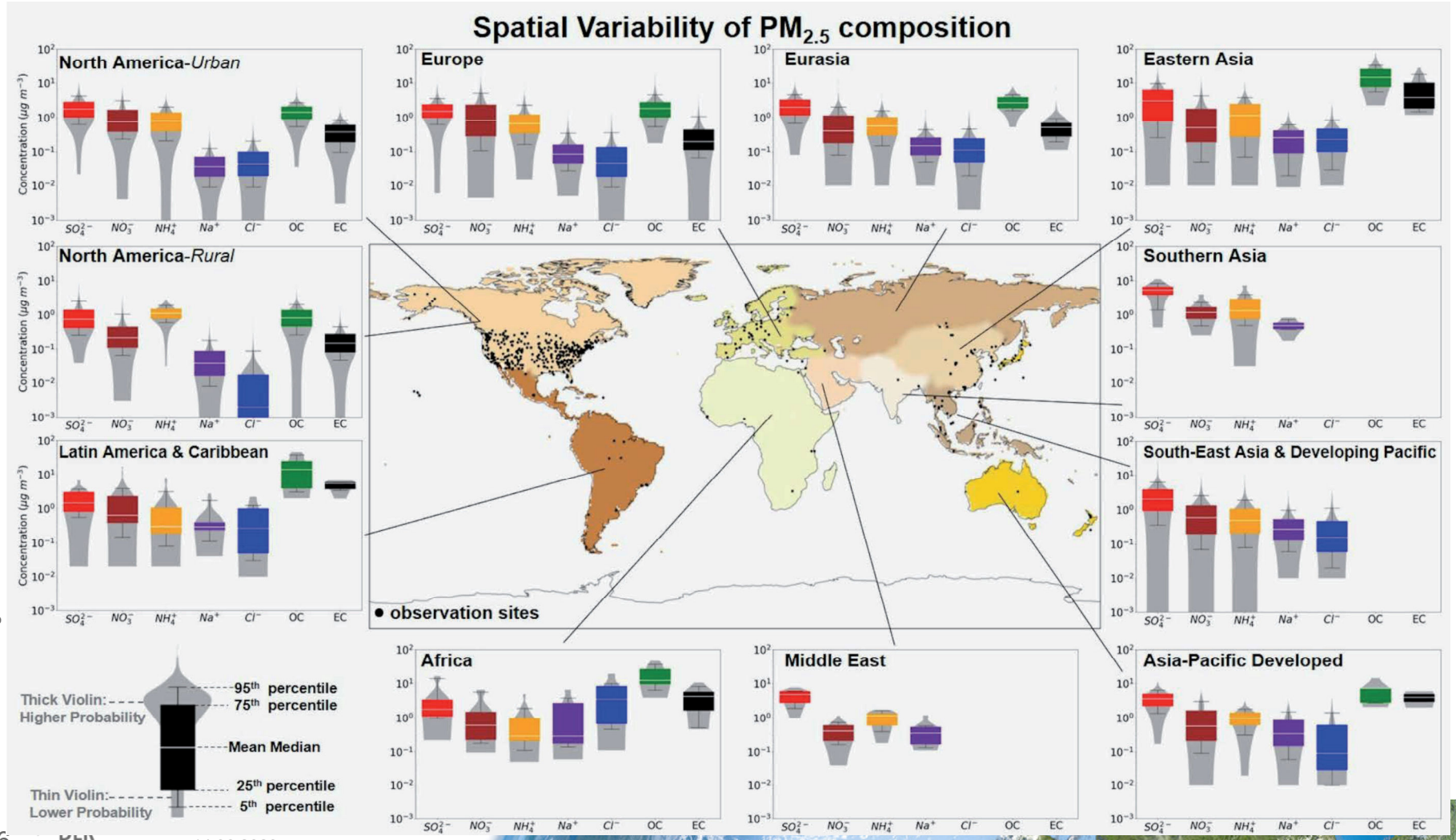

IPCC 2021, Chap. 6

Statements in the Executive Summary

Recent Evolution in Short-lived Climate Forcer (SLCF) (2)

There is no significant trend in the global mean tropospheric concentration of hydroxyl (OH) radical – the main sink for many SLCFs, including methane (CH_4) – from 1850 up to around 1980 (*low confidence*) but OH has remained stable or exhibited a positive trend since the 1980s (*medium confidence*). Global OH cannot be measured directly and is inferred from Earth system and chemistry–climate models (ESMs, CCMs) constrained by emissions and from observationally constrained inversion methods. There is conflicting information from these methods for the 1980–2014 period. ESMs and CCMs concur on a positive trend since 1980 (about a 9% increase over 1980–2014) and there is *medium confidence* that this trend is mainly driven by increases in global anthropogenic (human-caused) nitrogen oxide (NOx) emissions and decreases in anthropogenic CO emissions. The observation-constrained methods suggest either positive trends or the absence of trends based on *limited evidence* and *medium agreement*. Future changes in global OH, in response to SLCF emissions and climate change, will depend on the interplay between multiple offsetting drivers of OH. {6.3.6 and Cross-Chapter Box 5.1}

IPCC 2021, Chap. 6

Time evolution of global annual mean tropospheric hydroxyl (OH) over the historical period, expressed as a percentage anomaly relative to the mean over 1998–2007

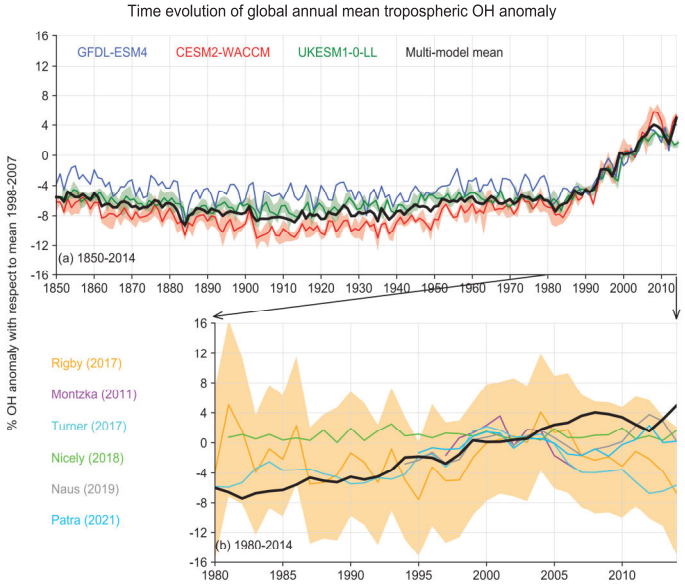

Figure 6.9 | Time evolution of global annual mean tropospheric hydroxyl (OH) over the historical period, expressed as a percentage anomaly relative to the mean over 1998–2007. (a) Results from three CMIP6 models, including UKESM1-0LL (green), GFDL-ESM4 (blue), and CESM2-WACCM (red), are shown; the shaded light green and light red bands show mean over multiple ensemble members for UKESM1-0LL (3) and CESM2-WACCM (3) models, respectively with the multi-model mean anomalies shown in thick black line. **(b)** Multi-model mean OH anomalies for the 1980–2014 period compared with those derived from observational-based inversions from Montzka et al., (2011); Rigby et al., (2017); Turner et al., (2017); Nicely et al., (2018); Naus et al., (2019); Patra et al., (2021) in the zoomed box. Further details on data sources and processing are available in the chapter data table (Table 6.SM.3).

IPCC 2021, Chap. 6

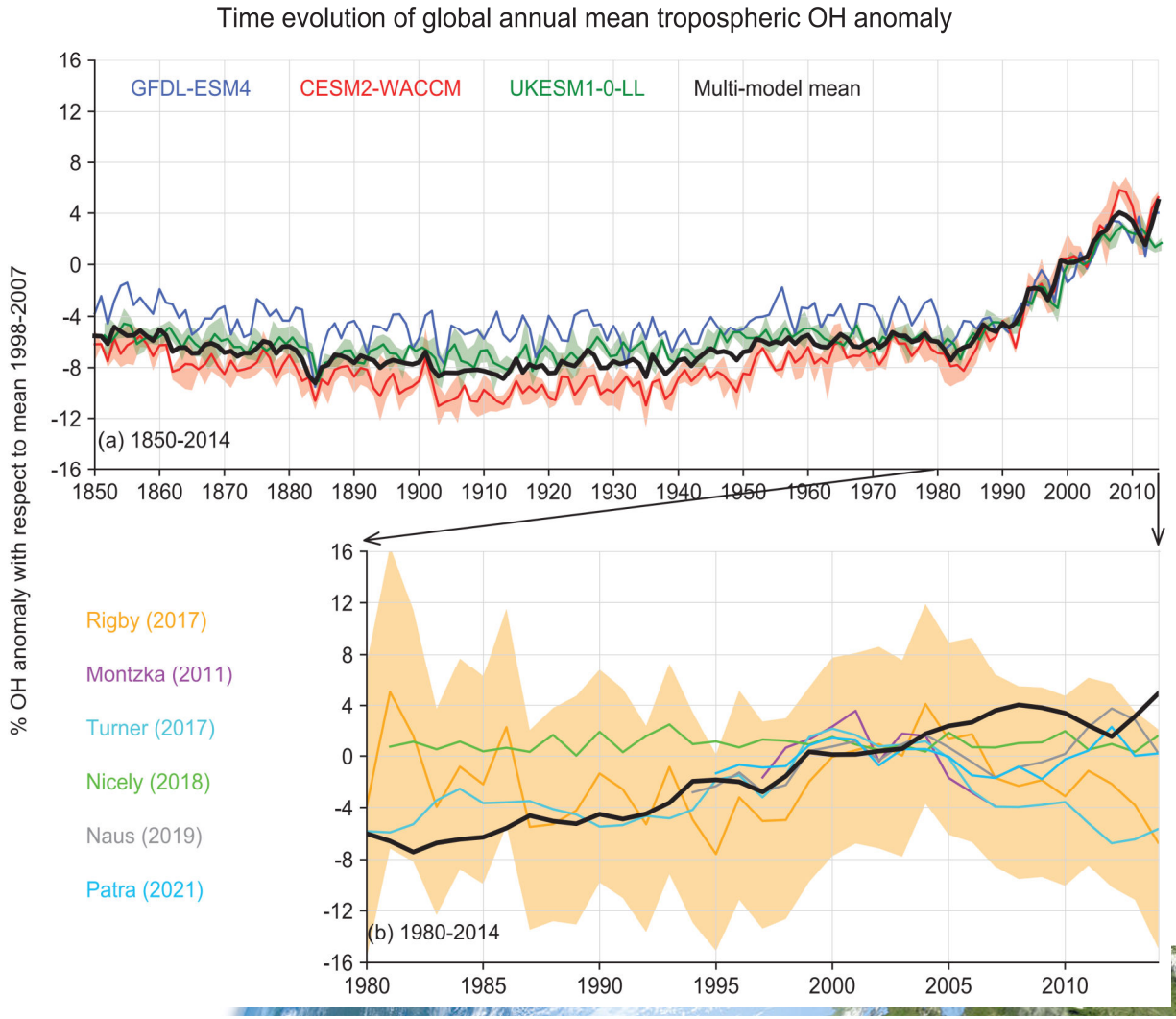

IPCC 2021, Chap. 6

Statements in the Executive Summary

Effect of SLCFs on Climate and Biogeochemical Cycles (1)

Over the historical period, changes in aerosols and their effective radiative forcing (ERF) have primarily contributed to a surface cooling, partly masking the greenhouse gas-driven warming (*high confidence*). Radiative forcings induced by aerosol changes lead to both local and remote temperature responses (*high confidence*). The temperature response preserves the south to north gradient of the aerosol ERF – hemispherical asymmetry – but is more uniform with latitude and is strongly amplified towards the Arctic (*medium confidence*). {6.4.1, 6.4.3}

Since the mid-1970s, trends in aerosols and their precursor emissions have led to a shift from an increase to a decrease of the magnitude of the negative globally averaged net aerosol ERF (*high confidence*). However, the timing of this shift varies by continental-scale region and has not occurred for some finer regional scales. The spatial and temporal distribution of the net aerosol ERF from 1850 to 2014 is highly heterogeneous, with stronger magnitudes in the Northern Hemisphere (*high confidence*). {6.4.1}

IPCC 2021, Chap. 6

Multi-model mean effective radiative forcings (ERFs) over the recent-past (1995-2014) induced by aerosol changes since 1850

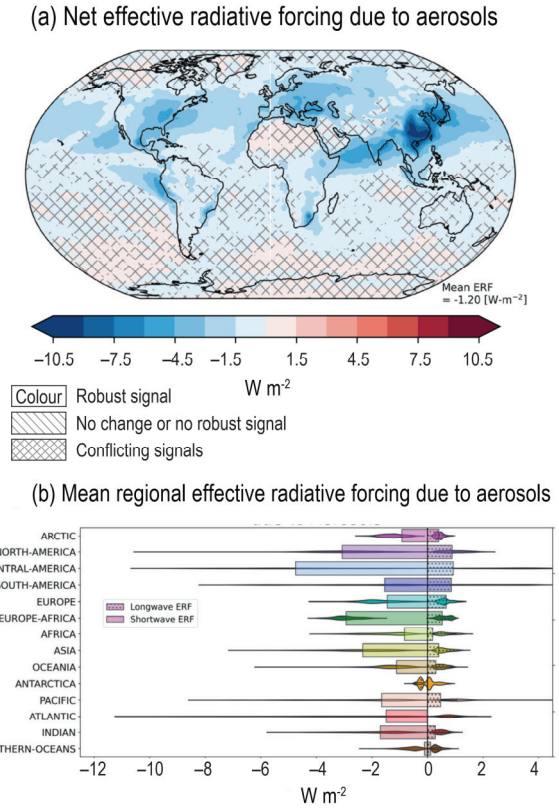

Figure 6.10 | Multi-model mean effective radiative forcings (ERFs) over the recent-past (1995-2014) induced by aerosol changes since 1850. Panel **(a)** shows the spatial distribution of the net ERF with area-weighted global mean ERF shown at the lower right corner. Uncertainty is represented using the advanced approach: no overlay indicates regions with robust signal, where ≥66% of models show change greater than variability threshold and ≥80% of all models agree on sign of change; diagonal lines indicate regions with no change or no robust signal, where <66% of models show a change greater than the variability threshold; crossed lines indicate regions with conflicting signal, where ≥66% of models show change greater than variability threshold and <80% of all models agree on sign of change. For more information on the advanced approach, please refer to the Cross-Chapter Box Atlas.1. Panel **(b)** shows the mean shortwave and longwave ERF for each of the 14 regions defined in the Atlas. Violins in panel (b) show the distribution of values over regions where ERFs are significant. ERFs are derived from the difference between top of the atmosphere (TOA) radiative fluxes for Aerosol Chemistry Model Intercomparison Project (AerChemMIP) experiments *histSST* and *histSST-piAer* (Collins et al., 2017) averaged over 1995–2014 (Box 1.4, Chapter 1). The results come from seven Earth system models: MIROC6, MPI-I-ESM-1-2-HAM, MRI-ESM2-0, GFDL-ESM4, GISS-E2-1-G, NorESM2-LM and UKESM-0-LL. These data can be seen in the Interactive Atlas. Further details on data sources and processing are available in the chapter data table (Table 6.SM.3).

Multi-model mean effective radiative forcings (ERFs) over the recent-past (1995-2014) induced by aerosol changes since 1850

(a) Net effective radiative forcing due to aerosols

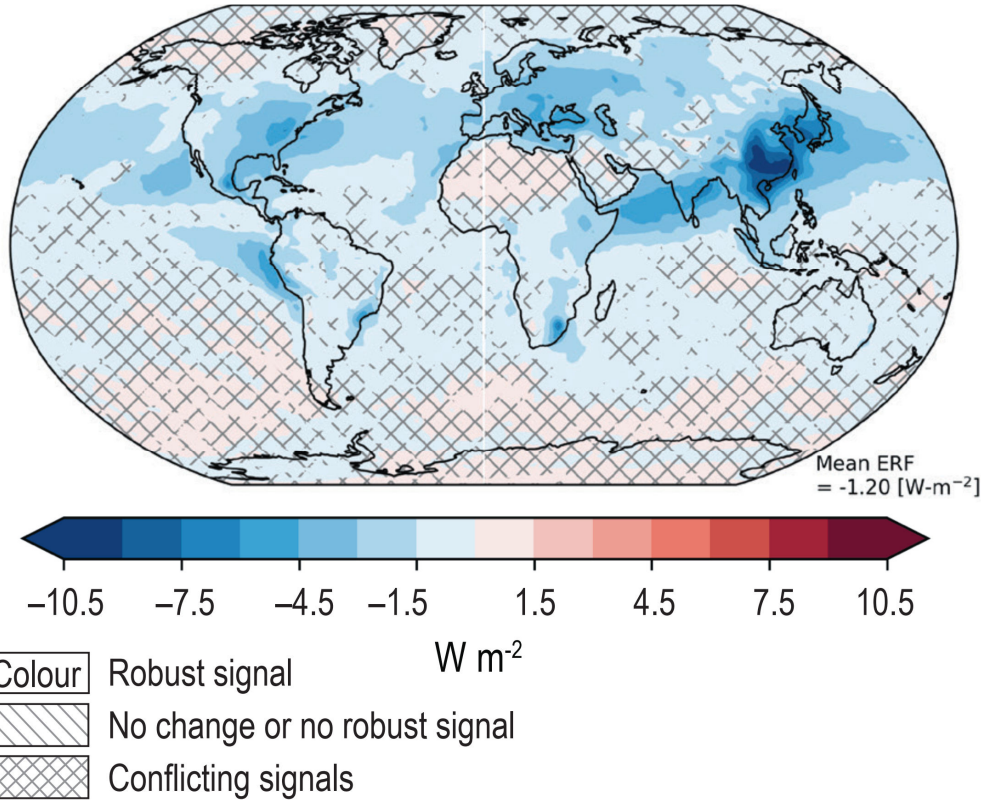

IPCC 2021, Chap. 6

Multi-model mean effective radiative forcings (ERFs) over the recent-past (1995-2014) induced by aerosol changes since 1850

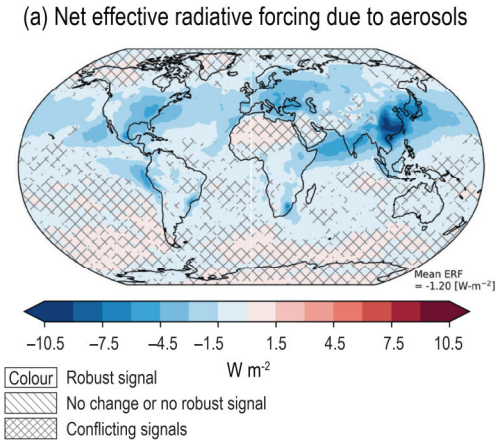

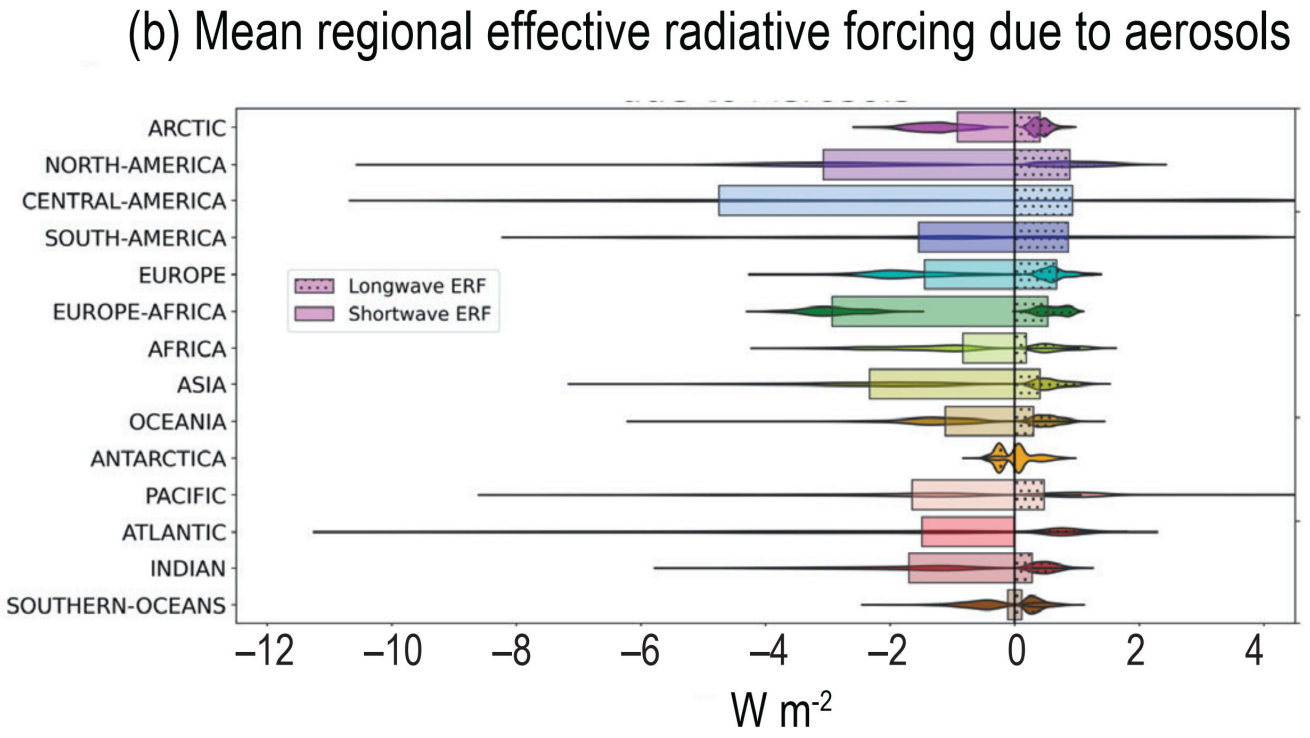

IPCC 2021, Chap. 6

Time evolution of 20-year multi-model mean averages of the annual area-weighted mean regional net effective radiative forcings (ERFs) due to aerosols for each of the 14 major regions in the Atlas, and global mean, using the models and model experiments as in Figure 6.10

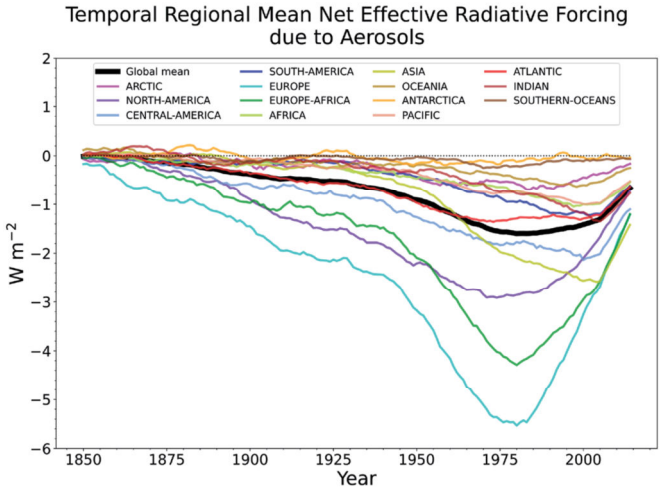

Figure 6.11 | Time evolution of 20-year multi-model mean averages of the annual area-weighted mean regional net effective radiative forcings (ERFs) due to aerosols for each of the 14 major regions in the Atlas, and global mean, using the models and model experiments as in Figure 6.10. Further details on data sources and processing are available in the chapter data table (Table 6.SM.3).

IPCC 2021, Chap. 6

Time evolution of 20-year multi-model mean averages of the annual area-weighted mean regional net effective radiative forcings (ERFs) due to aerosols for each of the 14 major regions in the Atlas, and global mean, using the models and model experiments as in Figure 6.10

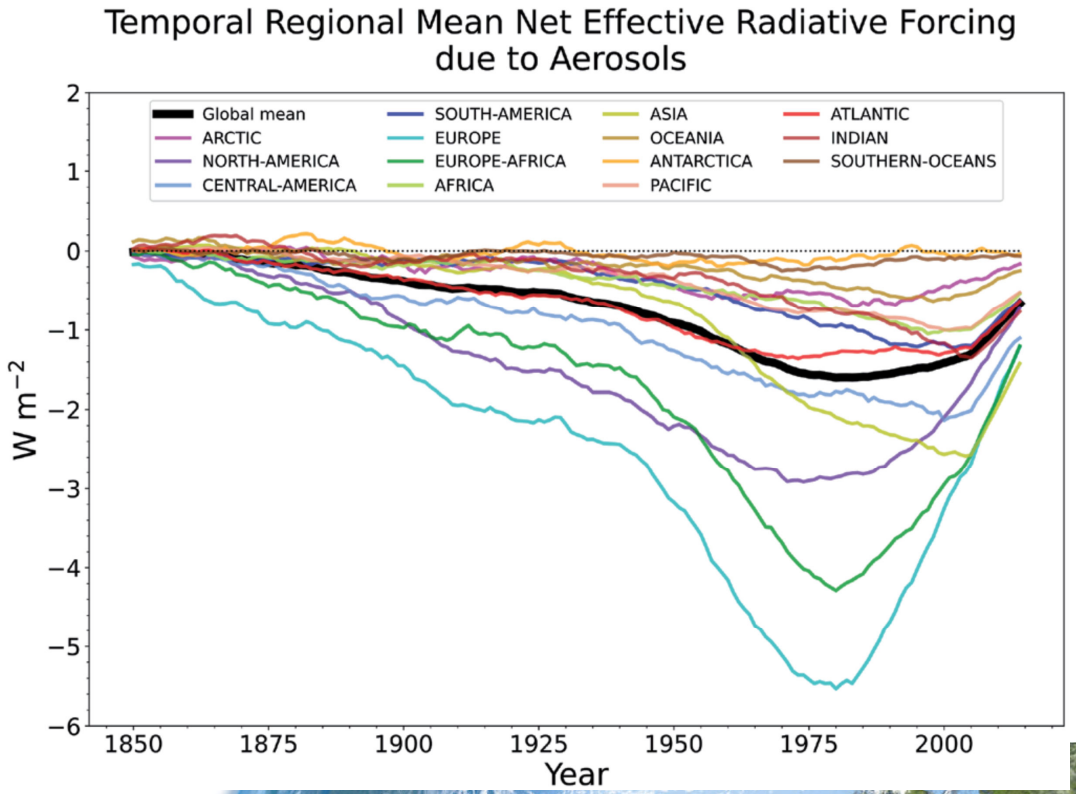

IPCC 2021, Chap. 6

Contribution to effective radiative forcing (ERF) (a) and global mean surface air temperature (GSAT) change (b) from component emissions between 1750 to 2019 based on CMIP6 models (Thornhill et al., 2021b)

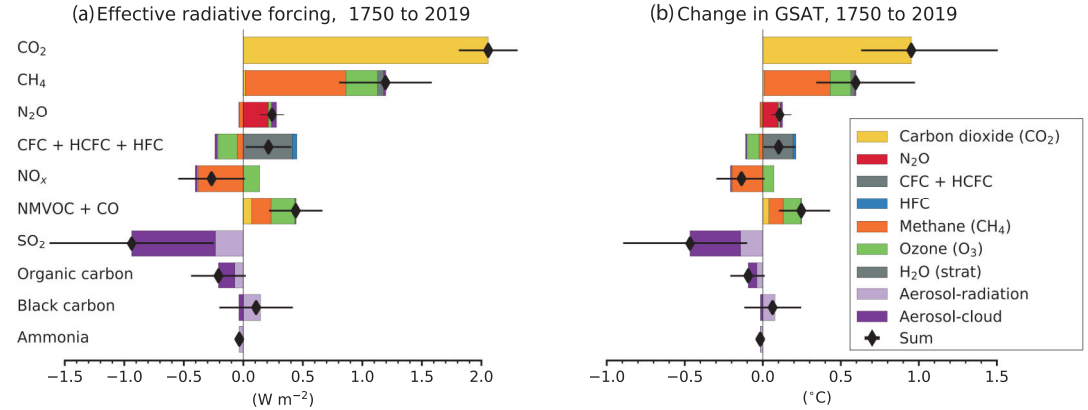

Figure 6.12 | Contribution to effective radiative forcing (ERF) (a) and global mean surface air temperature (GSAT) change (b) from component emissions between 1750 to 2019 based on CMIP6 models (Thornhill et al., 2021b). ERFs for the direct effect of well-mixed greenhouse gases (WMGHGs) are from the analytical formulae in section 7.3.2, H_2O (strat) is from Table 7.8. ERFs for other components are multi-model means from Thornhill et al. (2021b) and are based on ESM simulations in which emissions of one species at a time are increased from 1850 to 2014 levels. The derived emissions-based ERFs are rescaled to match the concentration-based ERFs in Figure 7.6. Error bars are 5–95% and for the ERF account for uncertainty in radiative efficiencies and multi-model error in the means. ERFs due to aerosol–radiation (ERFari) and cloud effects are calculated from separate radiation calls for clear-sky and aerosol-free conditions (Ghan, 2013; Thornhill et al., 2021b). 'Cloud' includes cloud adjustments (semi-direct effect) and ERF from indirect aerosol-cloud to –0.22 W m^{-2} for ERFari and –0.84 W m^{-2} interactions (ERFaci). The aerosol components (SO_2, organic carbon and black carbon) are scaled to sum to –0.22 W m^{-2} for ERFari and –0.84 W m^{-2} for 'cloud' (Section 7.3.3). For GSAT estimates, time series (1750–2019) for the ERFs have been estimated by scaling with concentrations for WMGHGs and with historical emissions for SLCFs. The time variation of ERFaci for aerosols is from Chapter 7. The global mean temperature response is calculated from the ERF time series using an impulse response function (Cross-Chapter Box 7.1) with a climate feedback parameter of –1.31 W m^{-2} $°C^{-1}$. Contributions to ERF and GSAT change from contrails and light-absorbing particles on snow and ice are not represented, but their estimates can be seen on Figure 7.6 and 7.7, respectively. Further details on data sources and processing are available in the chapter data table (Table 6.SM.3).

Contribution to effective radiative forcing (ERF) (a) and global mean surface air temperature (GSAT) change (b) from component emissions between 1750 to 2019 based on CMIP6 models (Thornhill et al., 2021b)

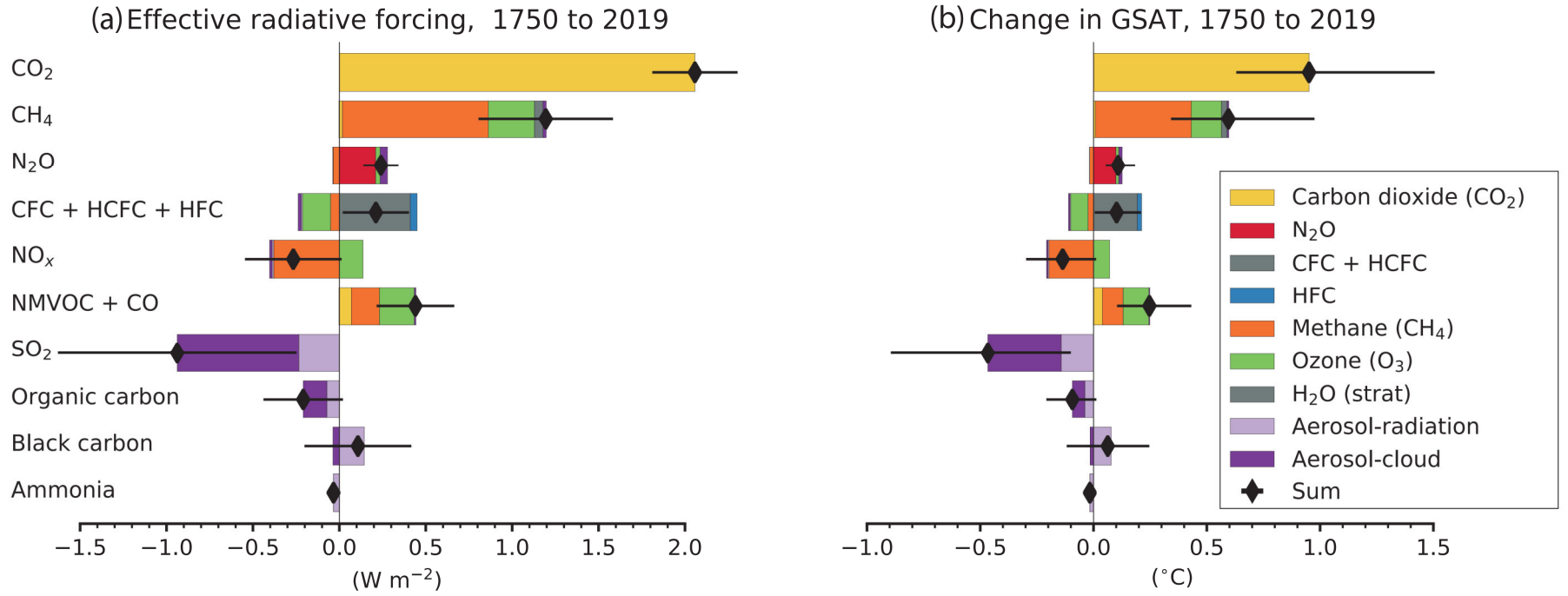

IPCC 2021, Chap. 6

Multi-model mean surface air temperature response over the recent past (1995–2014) induced by aerosol changes since 1850

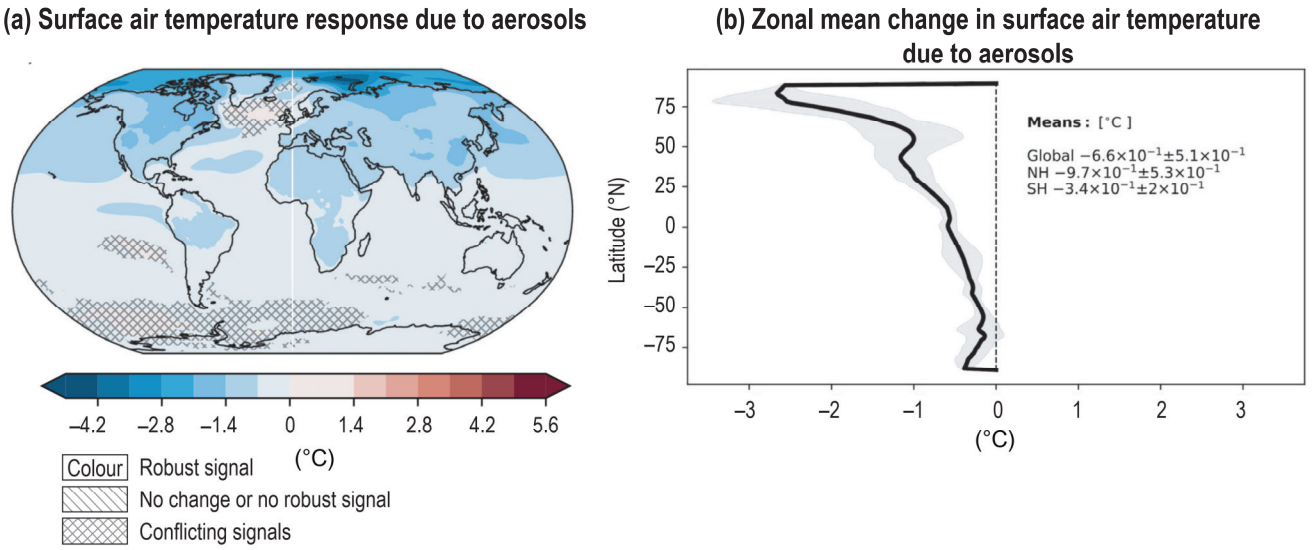

Figure 6.13 | Multi-model mean surface air temperature response over the recent past (1995–2014) induced by aerosol changes since 1850. Calculation is based on the difference between CMIP6 'historical' and AerChemMIP 'hist-piAer' experiments averaged over 1995–2014, where **(a)** is the spatial pattern of the annual mean surface air temperature response, and **(b)** is the mean zonally averaged response. Model means are derived from the years 1995–2014. Uncertainty is represented using the advanced approach: No overlay indicates regions with robust signal, where ≥66% of models show change greater than variability threshold and ≥80% of all models agree on sign of change; diagonal lines indicate regions with no change or no robust signal, where <66% of models show a change greater than the variability threshold; crossed lines indicate regions with conflicting signal, where ≥66% of models show change greater than variability threshold and <80% of all models agree on sign of change. For more information on the advanced approach, please refer to the Cross-Chapter Box Atlas.1. AerChemMIP models MIROC6, MRI-ESM2-0, NorESM2-LM, GFDL-ESM4, GISS-E2-1-G and UKESM1-0-LL are used in the analysis. Further details on data sources and processing are available in the chapter data table (Table 6.SM.3).

Multi-model mean surface air temperature response over the recent past (1995–2014) induced by aerosol changes since 1850

(a) Surface air temperature response due to aerosols

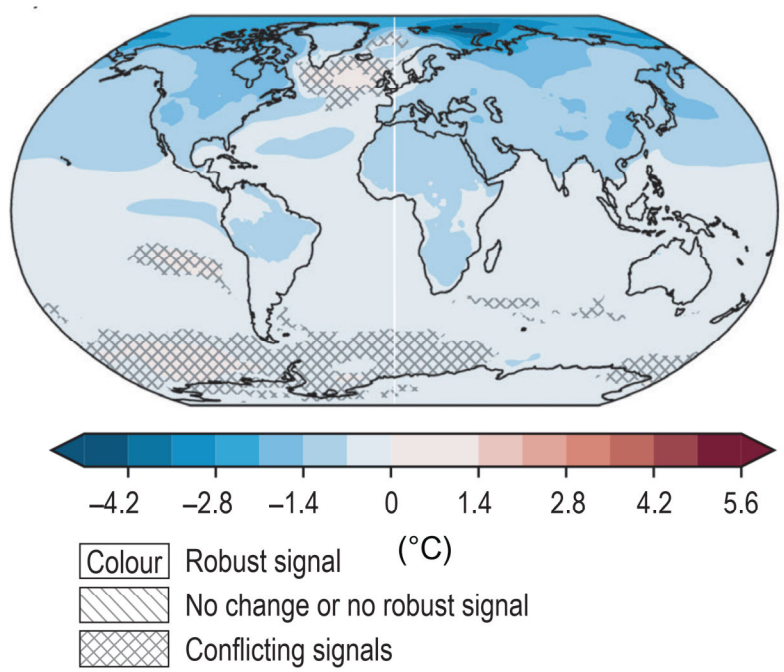

(b) Zonal mean change in surface air temperature due to aerosols

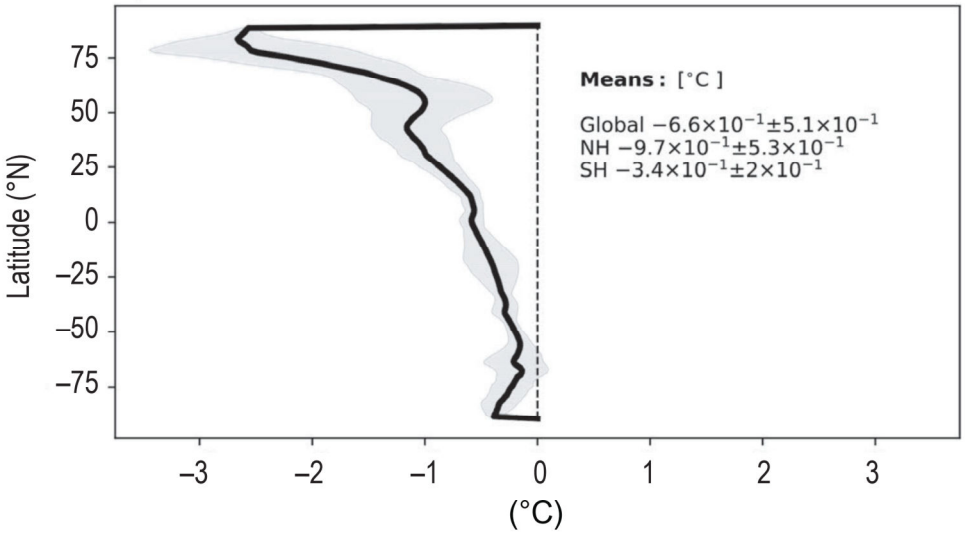

IPCC 2021, Chap. 6

Statements in the Executive Summary

Effect of SLCFs on Climate and Biogeochemical Cycles (2)

For forcers with short lifetimes (e.g., months) and not considering chemical adjustments, the response in surface temperature occurs strongly as soon as a sustained change in emissions is implemented, and that response continues to grow for a few years, primarily due to thermal inertia in the climate system (*high confidence*). Near its maximum, the response slows down but will then take centuries to reach equilibrium (*high confidence*). For SLCFs with longer lifetimes (e.g., a decade), a delay equivalent to their lifetimes is appended to the delay due to thermal inertia (*high confidence*). {6.6.1}

IPCC 2021, Chap. 6

Global mean surface air temperature (GSAT) response to an abrupt reduction in emissions (at time t=0) of idealized climate forcing agents with different lifetimes.

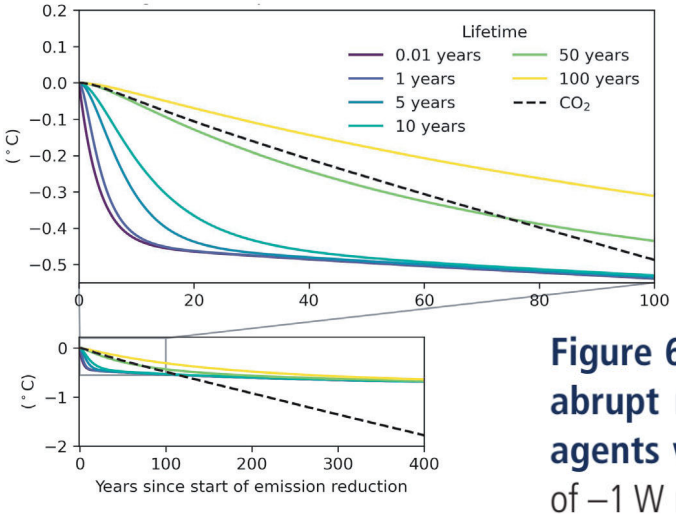

Figure 6.15 | Global mean surface air temperature (GSAT) response to an abrupt reduction in emissions (at time t=0) of idealized climate forcing agents with different lifetimes. All emissions are cut to give a radiative forcing of –1 W m^{-2} at a steady state (except for CO_2). In other words, if the yearly emissions are E_0 before the reduction, they will have a fixed lower value $E_{year>0} = (E_0 - \Delta E)$ for all succeeding years. For comparison, the GSAT response to a sustained reduction in CO_2 emissions resulting in an RF of –1 W m^{-2} in year 100 is included (dashed line). The temperature response is calculated using an impulse response function (Cross-Chapter Box 7.1) with a climate feedback parameter of –1.31 W m^{-2} °C^{-1}. Further details on data sources and processing are available in the chapter data table (Table 6. SM.3).

IPCC 2021, Chap. 6

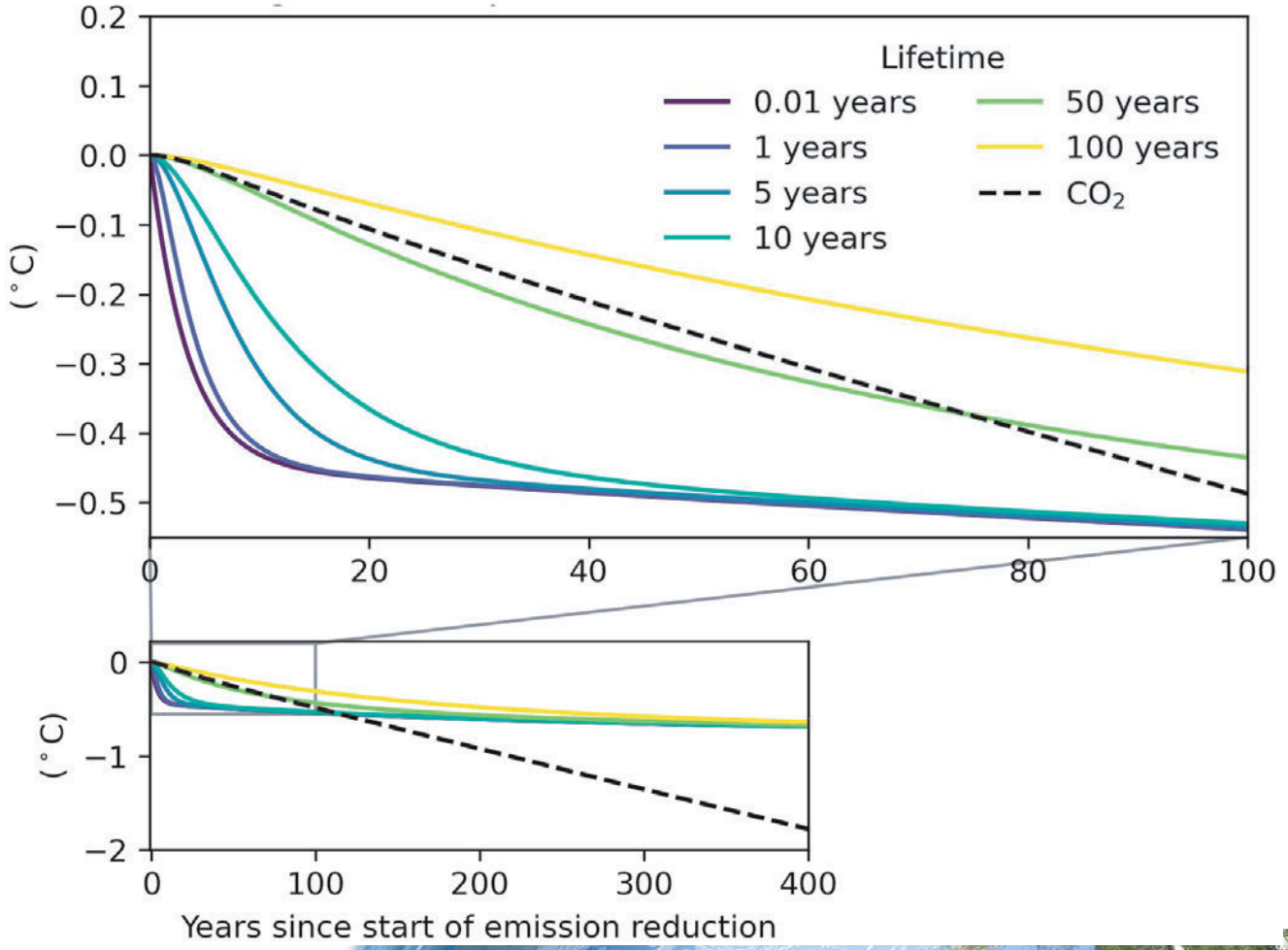

IPCC 2021, Chap. 6

Global mean temperature response 10 and 100 years following one year of present-day (year 2014) emissions

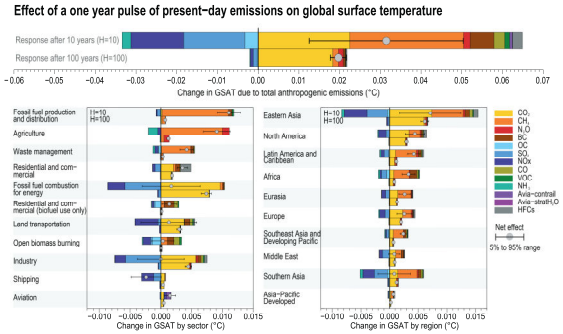

Figure 6.16 | Global mean temperature response 10 and 100 years following one year of present-day (year 2014) emissions. The temperature response is broken down by individual species and shown for total anthropogenic emissions (top), sectoral emissions (left) and regional emissions (right). Sectors and regions are sorted by (high-to-low) net temperature effect on the 10-year time scale. Error bars in the top panel show uncertainty (5–95% interval) in net temperature effect due to uncertainty in radiative forcing *only* (calculated using a Monte Carlo approach and best estimate uncertainties from the literature – see Lund et al. (2020) for details). CO_2 emissions are excluded from open biomass burning and residential biofuel use due to their unavailability in the Community Emissions Data System (CEDS) and uncertainties around non-sustainable emission fraction. Emissions for 2014 originate from the CEDS (Hoesly et al., 2018), except for HFCs which are from Purohit et al. (2020), open biomass burning from van Marle et al. (2017), and aviation H_2O which is from Lee et al. (2021). The split of fossil fuel production and distribution and combustion for energy and residential and commercial fuel use into fossil fuel and biofuel components is obtained from the GAINS model (ECLIPSE version 6b dataset). Open biomass burning emissions are not included for the regions. Emissions are aggregated into fossil fuel production and distribution (coal mining, oil and gas production, upstream gas flaring and gas distribution networks), agriculture (livestock and crop production), fossil fuel combustion for energy (power plants), industry (combustion and production processes, solvent-use losses from production and end use), residential and commercial (fossil fuel use for cooking and heating as well is HFCs leakage from A/C and refrigeration), waste management (solid waste, including landfills and open trash burning, residential and industrial waste water), transport (road and off-road vehicles, and HFC leakage from A/C and refrigeration equipment), residential and commercial (biofuels use for cooking and heating), open biomass burning (forest, grassland, savanna fires and agricultural waste burning), shipping (including international shipping), and aviation (including international aviation). Further details on data sources and processing are available in the chapter data table (Table 6. SM.3).

Effect of a one year pulse of present−day emissions on global surface temperature

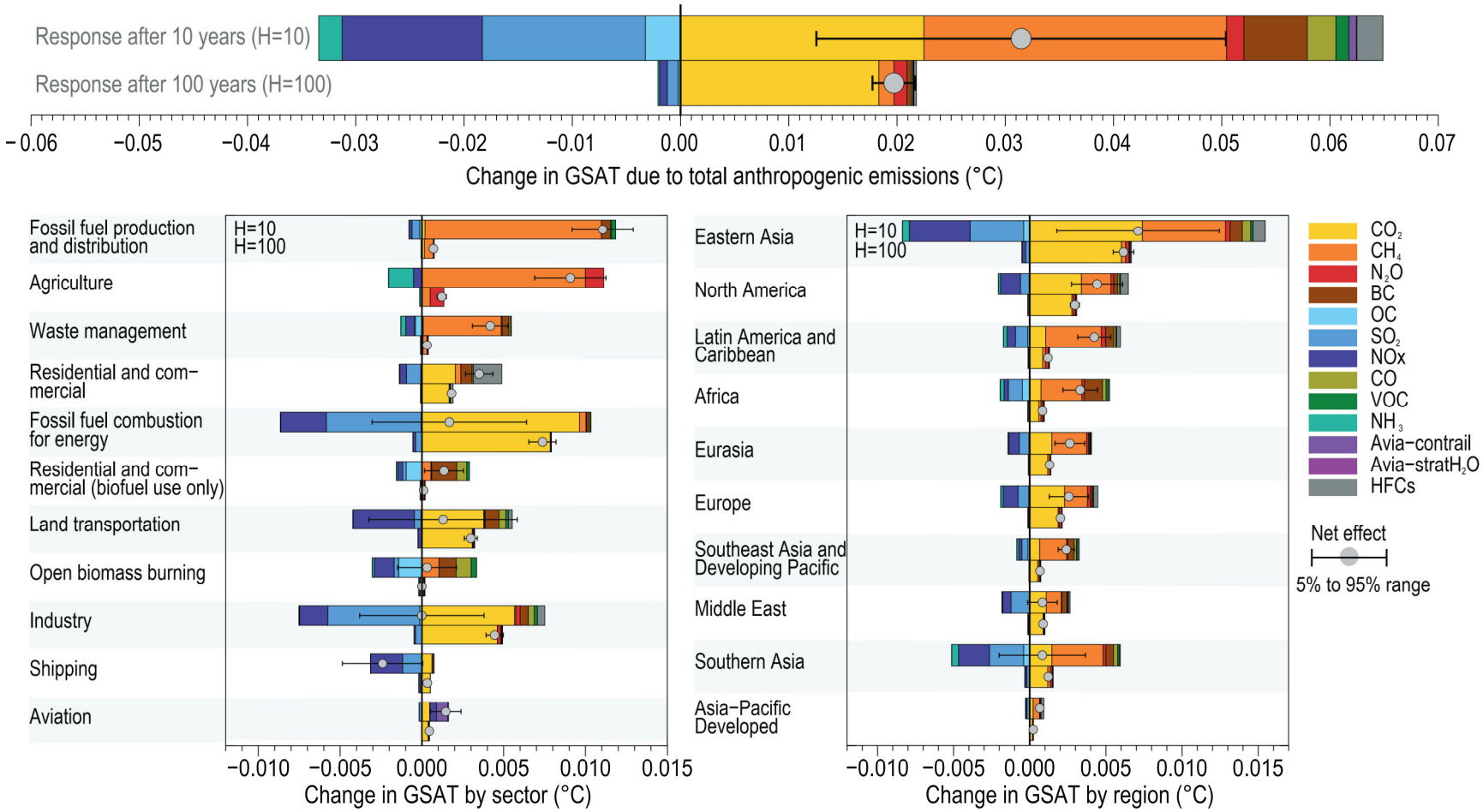

IPCC 2021, Chap. 6

Statements in the Executive Summary

Effect of SLCFs on Climate and Biogeochemical Cycles (3)

Over the 1750–2019 period, changes in SLCF emissions, especially of methane, NO_x and SO_2, have substantial effects on effective radiative forcing (ERF) (*high confidence*). The net global emissions-based ERF of NO_x is negative and that of non-methane volatile organic compounds (NMVOCs) is positive, in agreement with the AR5 Assessment (*high confidence*). For methane, the emissions-based ERF is twice as high as the abundance-based ERF (*high confidence*) attributed to chemical adjustment mainly via ozone production. SO_2 emissions changes make the dominant contribution to the ERF from aerosol–cloud interactions (*high confidence*). Over the 1750–2019 period, the contributions from the emitted compounds to changes in global surface air temperature (GSAT) broadly match their contributions to the ERF (*high confidence*). Since a peak in emissions-induced SO_2 ERF has already occurred recently and since there is a delay in the full GSAT response, changes in SO_2 emissions have a slightly larger contribution to GSAT change than CO_2 emissions, relative to their respective contributions to ERF. {6.4.2, 6.6.1 and 7.3.5}

IPCC 2021, Chap. 6

Statements in the Executive Summary

Effect of SLCFs on Climate and Biogeochemical Cycles (4)

Reactive nitrogen, ozone and aerosols affect terrestrial vegetation and the carbon cycle through deposition and effects on large-scale radiation (*high confidence*). However, the magnitude of these effects on the land carbon sink, ecosystem productivity and hence their indirect CO_2 forcing remain uncertain due to the difficulty in disentangling the complex interactions between the individual effects. As such, these effects are assessed to be of second order in comparison to the direct CO_2 forcing (*high confidence*), but effects of ozone on terrestrial vegetation could add a substantial (positive) forcing compared with the direct ozone forcing (*low confidence*). {6.4.4}

IPCC 2021, Chap. 6

Statements in the Executive Summary

Effect of SLCFs on Climate and Biogeochemical Cycles (5)

Climate feedbacks induced from changes in emissions, abundances or lifetimes of SLCFs mediated by natural processes or atmospheric chemistry are assessed to have an overall cooling effect (*low confidence*), that is, a total negative feedback parameter of –0.20 [–0.41 to +0.01] W m^{-2} $^{o}C^{-1}$. These non-CO_2 biogeochemical feedbacks are estimated from ESMs, which have advanced since AR5 to include a consistent representation of biogeochemical cycles and atmospheric chemistry. However, process-level understanding of many chemical and biogeochemical feedbacks involving SLCFs, particularly natural emissions, is still emerging, resulting in low confidence in the magnitude and sign of most SLCF climate feedback parameters. {6.2.2, 6.4.5}

IPCC 2021, Chap. 6

Statements in the Executive Summary

Future Projections for Air Quality Considering Shared Socio-economic Pathways (SSPs) (1)

Future air quality (in term of surface ozone and PM concentrations) on global to local scales will be primarily driven by changes in precursor emissions as opposed to climate change (*high confidence*) and climate change is projected to have mixed effects. A warmer climate is expected to reduce surface ozone in regions remote from pollution sources (*high confidence*) but is expected to increase it by a few parts per billion over polluted regions, depending on ozone precursor levels (*medium to high confidence*). Future climate change is expected to have mixed effects, positive or negative, with an overall low effect, on global surface PM and more generally on the aerosol global burden (*medium confidence*), but stronger effects are not excluded in regions prone to specific meteorological conditions (*low confidence*). Overall, there is *low confidence* in the response of surface ozone and PM to future climate change due to the uncertainty in the response of the natural processes (e.g., stratosphere–troposphere exchange, natural precursor emissions, particularly including biogenic volatile organic compounds, wildfire-emitted precursors, land and marine aerosols, and lightning NOx) to climate change. {6.3, 6.5}

IPCC 2021, Chap. 6

Statements in the Executive Summary

Future Projections for Air Quality Considering Shared Socio-economic Pathways (SSPs) (2)

The SSPs span a wider range of SLCF emissions than the Representative Concentration Pathways (RCPs), representing better the diversity of future options in air pollution management (*high confidence*). In the SSPs, the socio-economic assumptions and climate change mitigation levels primarily drive future emissions, but the SLCF emissions trajectories are also steered by varying levels of air pollution control originating from the SSP narratives, independently from climate change mitigation. Consequently, SSPs consider a large variety of regional ambitions and effectiveness in implementing air pollution legislation and result in wider range of future air pollution levels and SLCF-induced climate effects. {6.7.1}

IPCC 2021, Chap. 6

Statements in the Executive Summary

Future Projections for Air Quality Considering Shared Socio-economic Pathways (SSPs) (3)

Air pollution projections range from strong reductions in global surface ozone and PM (e.g., SSP1-2.6, with strong mitigation of both air pollution and climate change) to no improvement and even degradation (e.g., SSP3-7.0 without climate change mitigation and with only weak air pollution control) (*high confidence*). Under the SSP3-7.0 scenario, PM levels are projected to increase until 2050 over large parts of Asia, and surface ozone pollution is projected to worsen over all continental areas through 2100 (*high confidence*). Without climate change mitigation but with stringent air pollution control (SSP5-8.5), PM levels decline through 2100, but high methane levels hamper the decline in global surface ozone at least until 2080 (*high confidence*). {6.7.1}

IPCC 2021, Chap. 6

Statements in the Executive Summary

Future Projections of the Effect of SLCFs on GSAT in the Core SSPs (1)

In the next two decades, it is *very likely* that the SLCF emissions changes in the WGI core set of SSPs will cause a warming relative to 2019, whatever the SSPs, in addition to the warming from long-lived greenhouse gases. The net effect of SLCF and hydrofluorocarbon (HFC) changes on GSAT across the SSPs is a *likely* warming of 0.06°C–0.35°C in 2040 relative to 2019. Warming over the next two decades is quite similar across the SSPs due to competing effects of warming (methane, ozone) and cooling (aerosols) SLCFs. For the scenarios with the most stringent climate and air pollution mitigations (SSP1-1.9 and SSP1-2.6), the likely near-term warming from the SLCFs is predominantly due to sulphate aerosol reduction, but this effect levels off after 2040. In the absence of climate change policies and with weak air pollution control (SSP3-7.0), the likely near-term warming due to changes in SLCFs is predominantly due to increases in methane, ozone and HFCs, with smaller contributions from changes in aerosols. SSP5-8.5 has the highest SLCF-induced warming rates due to warming from methane and ozone increases and reduced aerosols due to stronger air pollution control compared to the SSP3-7.0 scenario

IPCC 2021, Chap. 6

Statements in the Executive Summary

Future Projections of the Effect of SLCFs on GSAT in the Core SSPs (2)

At the end of the century, the large diversity of GSAT response to SLCF changes among the scenarios robustly covers the possible futures, as the scenarios are internally consistent and span a range from very high to very low emissions. In the scenarios without climate change mitigation (SSP3-7.0 and SSP5-8.5) the *likely* range of the estimated warming due to SLCFs in 2100 relative to 2019 is 0.4°C–0.9°C {6.7.3, 6.7.4}. In SSP3-7.0 there is a near-linear warming due to SLCFs of 0.08°C per decade, while for SSP5-8.5 there is a more rapid warming in the first half of the century. For the scenarios considering the most stringent climate and air pollution mitigations (SSP1-1.9 and SSP1-2.6), the reduced warming from reductions in methane, ozone and HFCs partly balances the warming from reduced aerosols, and the overall SLCF effect is a *likely* increase in GSAT of 0.0°C–0.3°C in 2100, relative to 2019. The SSP2-4.5 scenario (with moderate climate change and air pollution mitigations) results in a *likely* warming of 0.2°C–0.5°C in 2100 due to SLCFs, with the largest warming from reductions in aerosols. {6.7.3}

IPCC 2021, Chap. 6

Time evolution of the effects of changes in short-lived climate forcers (SLCFs) and hydrofluorocarbons (HFCs) on global surface air temperature (GSAT) across the WGI core set of Shared Socio-Economic Pathways (SSPs)

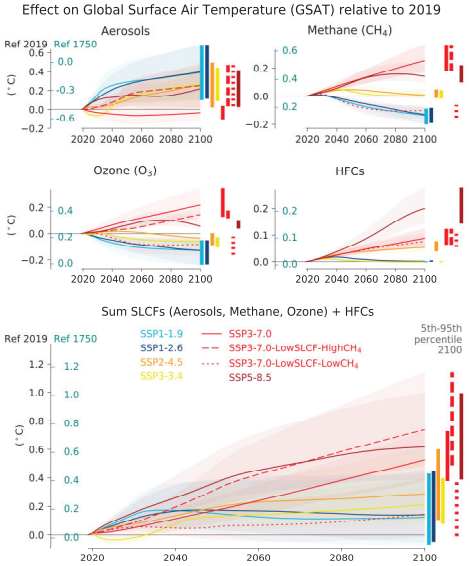

Figure 6.22 | Time evolution of the effects of changes in short-lived climate forcers (SLCFs) and hydrofluorocarbons (HFCs) on global surface air temperature (GSAT) across the WGI core set of Shared Socio-Economic Pathways (SSPs). Effects of net aerosols, methane, tropospheric ozone and hydrofluorocarbons (HFCs; with lifetimes <50years), and the sum of these, relative to the year 2019 and to the year 1750. The GSAT changes are based on the assessed historic and future evolution of effective radiative forcing (ERF; Section 7.3.5). The temperature responses to the ERFs are calculated with an impulse response function with an equilibrium climate sensitivity of 3.0°C for a doubling of atmospheric CO_2 (feedback parameter of -1.31 W m^{-2} °C^{-1}, see Cross-Chapter Box 7.1). The vertical bars to the right in each panel show the uncertainties (5–95% ranges) for the GSAT change between 2019 and 2100. Further details on data sources and processing are available in the chapter data table (Table 6.SM.3).

IPCC 2021, Chap. 6

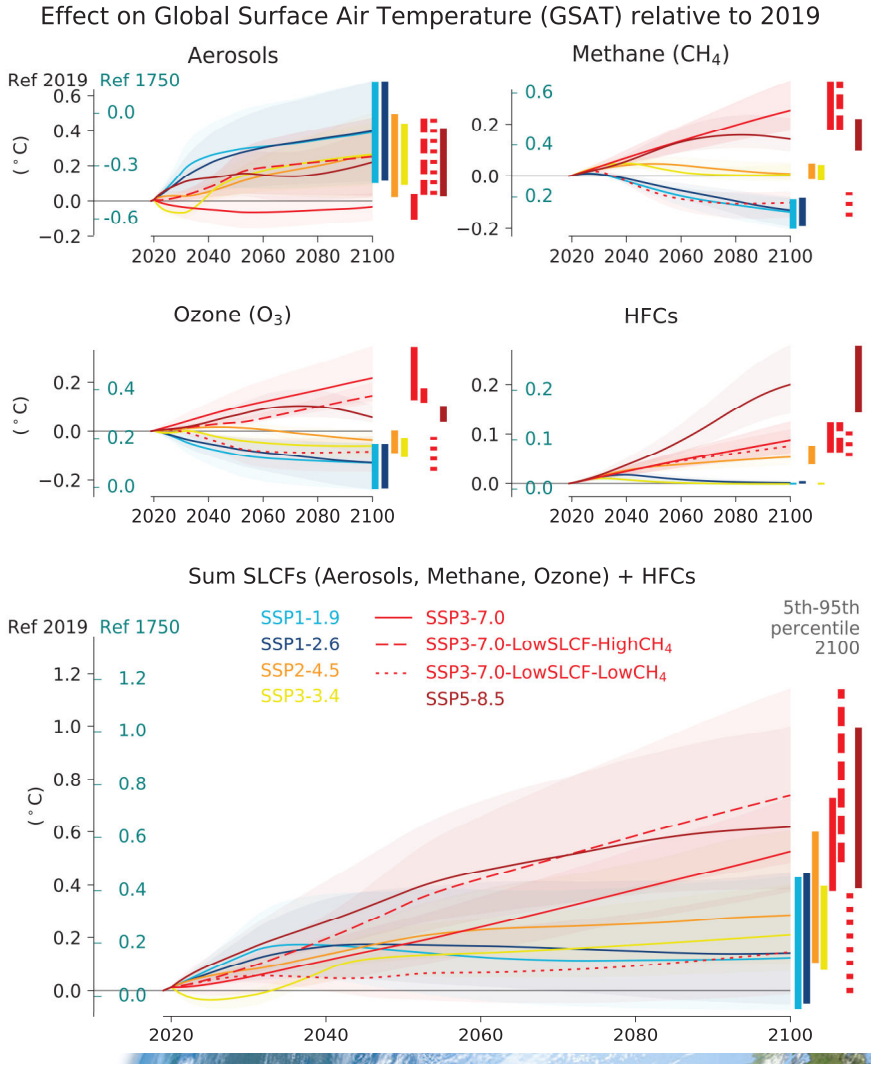

IPCC 2021, Chap. 6

Statements in the Executive Summary

Potential Effects of SLCF Mitigation (1)

Over time scales of 10 to 20 years, the global temperature response to a year's worth of current emissions of SLCFs is at least as large as that due to a year's worth of CO_2 emissions (*high confidence*). Sectors producing the largest SLCF-induced warming are those dominated by methane emissions: fossil fuel production and distribution, agriculture and waste management (*high confidence*). On these time scales, SLCFs with cooling effects can significantly mask the CO_2 warming in the case of fossil fuel combustion for energy and land transportation, or completely offset the CO_2 warming and lead to an overall net cooling in the case of industry and maritime shipping (prior to the implementation of the revised fuel-sulphur limit policy for shipping in 2020) (*medium confidence*). Ten years after a one-year pulse of present-day aviation emissions, SLCFs induce strong but short-lived warming contributions to the GSAT response (*medium confidence*), while CO_2 both gives a warming effect in the near term and dominates the long-term warming impact (*high-confidence*). {6.6.1, 6.6.2}

IPCC 2021, Chap. 6

Statements in the Executive Summary

Potential Effects of SLCF Mitigation (2)

The effects of SLCFs decay rapidly over the first few decades after pulse emission. Consequently, on time scales longer than about 30 years, the net long-term global temperature effects of sectors and regions are dominated by CO_2 (*high confidence*). The global mean temperature response following a climate change mitigation measure that affects emissions of both short- and long-lived climate forcers depends on their atmospheric decay times, how fast and for how long the emissions are reduced, and the inertia in the climate system. For SLCFs including methane, the rate of emissions drives the long-term global temperature effect, as opposed to CO_2 for which the long-term global temperature effect is controlled by the cumulative emissions. About 30 years or more after a one-year emission pulse occurs, the sectors contributing the most to global warming are industry, fossil fuel combustion for energy and land transportation, essentially through CO_2 (*high confidence*). Current emissions of SLCFs, CO_2 and N_2O from Eastern Asia and North America are the largest regional contributors to additional net future warming on both short (medium confidence) and long time scales (*high confidence*). {6.6.1, 6.6.2}

IPCC 2021, Chap. 6

Statements in the Executive Summary

Potential Effects of SLCF Mitigation (3)

At present, emissions from the residential and commercial sectors (fossil and biofuel use for cooking and heating) and the energy sector (fossil fuel production, distribution and combustion) contribute the most to the world population's exposure to anthropogenic fine PM (*high confidence*), whereas emissions from the energy and land transportation sectors contribute the most to ozone exposure (*medium to high confidence*). The contribution of different sectors to PM varies across regions, with the residential sector being the most important in Southern Asia and Africa, agricultural emissions dominating in Europe and North America, and industry and energy production dominating in Central and Eastern Asia, Latin America and the Middle East. Energy and industry are important PM2.5 contributors in most regions, except Africa (*high confidence*). Sector contributions to surface ozone concentrations are similar for all regions. {6.6.2}

IPCC 2021, Chap. 6

Statements in the Executive Summary

Potential Effects of SLCF Mitigation (4)

Assuming implementation and efficient enforcement of both the Kigali Amendment to the Montreal Protocol on Ozone Depleting Substances and current national plans to limit emissions (as in SSP1-2.6), the effects of HFCs on GSAT, relative to 2019, would remain below +0.02°C from 2050 onwards versus about +0.04°C to +0.08°C in 2050 and +0.1°C to +0.3°C in 2100 considering only national HFC regulations decided prior to the Kigali Amendment (as in SSP5-8.5) (*medium confidence*). Further improvements in the efficiency of refrigeration and air-conditioning equipment during the transition to low-global-warming-potential refrigerants would bring additional greenhouse gas reductions (*medium confidence*) resulting in benefits for climate change mitigation and to a lesser extent for air quality due to reduced air pollutant emissions from power plants. {6.6.3, 6.7.3}

IPCC 2021, Chap. 6

Statements in the Executive Summary

Potential Effects of SLCF Mitigation (5a)

Future changes in SLCFs are expected to cause additional warming. This warming is stable after 2040 in scenarios leading to lower global air pollution as long as methane emissions are also mitigated, but the overall warming induced by SLCF changes is higher in scenarios in which air quality continues to deteriorate (induced by growing fossil fuel use and limited air pollution control) (*high confidence*). If a strong air pollution control resulting in reductions in anthropogenic aerosols and non-methane ozone precursors was considered in SSP3-7.0, it would lead to a likely additional near-term global warming of 0.08 [0.00 to 0.10] °C in 2040. An additional concomitant methane mitigation (consistent with SSP1's stringent climate change mitigation policy implemented in the SSP3 world) would not only alleviate this warming but would turn this into a cooling of 0.07°C with a likely range of [–0.02 to +0.14] °C (compared with SSP3-7.0 in 2040). ...

IPCC 2021, Chap. 6

Statements in the Executive Summary

Potential Effects of SLCF Mitigation (5b)

... Across the SSPs, the collective reduction of methane, ozone precursors and HFCs can make a difference of 0.2°C with a very likely range of [0.1 to 0.4] °C in 2040 and 0.8°C with a very likely range of [0.5 to 1.3] °C at the end of the 21st century (comparing SSP3-7.0 and SSP1-1.9), which is substantial in the context of the Paris Agreement. Sustained methane mitigation, wherever it occurs, stands out as an option that combines near- and long-term gains on surface temperature (high confidence) and leads to air-quality benefits by reducing surface ozone levels globally (high confidence). {6.6.3, 6.7.3, 4.4.4}

IPCC 2021, Chap. 6

Statements in the Executive Summary

Potential Effects of SLCF Mitigation (6)

Rapid decarbonization strategies lead to air-quality improvements but are not sufficient to achieve, in the near term, air-quality guidelines set for fine PM by the World Health Organization (WHO), especially in parts of Asia and in some other highly polluted regions (*high confidence*). Additional methane and BC mitigation would contribute to offsetting the additional warming associated with SO_2 reductions that would accompany decarbonization (*high confidence*). Strong air pollution control as well as strong climate change mitigation, implemented separately, lead to large reductions in exposure to air pollution by the end of the century (*high confidence*). Implementation of air pollution controls, relying on the deployment of existing technologies, leads more rapidly to air quality benefits than climate change mitigation (*high confidence*), which requires systemic changes. However, in both cases, significant parts of the population are projected to remain exposed to air pollution exceeding the WHO guidelines (*high confidence*). Additional policies envisaged to attain Sustainable Development Goals (SDGs; e.g., access to clean energy, waste management) bring complementary SLCF reduction. Only strategies integrating climate, air quality, and development goals are found to effectively achieve multiple benefits. {6.6.3, 6.7.3, Box 6.2}

Statements in the Executive Summary

Implications of COVID-19 Restrictions for Emissions, Air Quality and Climate

Emissions reductions associated with COVID-19 containment led to a discernible temporary improvement of air quality in most regions, but changes to global and regional climate are undetectable above internal variability. Global anthropogenic NO_x emissions decreased by a maximum of about 35% in April 2020 (*medium confidence*). There is *high confidence* that, with the exception of surface ozone, these emissions reductions have contributed to improved air quality in most regions of the world. Global fossil CO_2 emissions decreased by 7% (with a range of 5.8–13.0%) in 2020 relative to 2019, largely due to reduced emissions from the transportation sector (medium confidence). Overall, the net ERF, relative to ongoing trends, from COVID-19 restrictions was likely small and positive for 2020 (less than 0.2 W m^{-2}), thus temporarily adding to the total anthropogenic climate influence, with positive forcing from aerosol changes dominating over negative forcings from CO_2, NO_x and contrail cirrus changes. Consistent with this small net radiative forcing, and against a large component of internal variability, Earth system model simulations show no detectable effect on global or regional surface temperature or precipitation (high confidence). {Cross-Chapter Box 6.1}

IPCC 2021, Chap. 6